9592 *Macromolecules* **2009**, *42*, 9592–9608
DOI: 10.1021/ma900950s

Macromolecules
ARTICLE

Stress Relaxation of Comb Polymers with Short Branches

Keith M. Kirkwood and L. Gary Leal*

Department of Chemical Engineering, University of California, Santa Barbara, Santa Barbara, California 93106

Dimitris Vlassopoulos

Institute of Electronic Structure & Laser, FORTH, Heraklion 71110, Crete, Greece and Department of Materials Science & Technology, University of Crete, Heraklion 71003, Crete, Greece

Paraskevi Driva and Nikos Hadjichristidis

Department of Chemistry, University of Athens, Panepistimiopolis Zografou 15771 Athens, Greece

Received April 30, 2009; Revised Manuscript Received October 29, 2009

ABSTRACT: We measured the linear and nonlinear rheology of model polyisoprene comb polymers with a moderate number (5−18) of short (marginally entangled to unentangled) branches and highly entangled backbones. The hierarchical modes of relaxation were found to govern both the linear and nonlinear response. Appropriate modification of tube-model theory for entangled branches, inspired by recent work on asymmetric star polymers (where the short branch behaves as effectively larger on small time scales), provided a framework for quantitative predictions of the linear viscoelastic spectra. The extended nonlinear stress relaxation data over a wide time range (via time−temperature superposition) obeys time−strain separability and allows extraction of two damping functions: one for the branches at short times and one for the diluted backbone at long times. Both exhibit signatures of the comb architecture. The comb damping function at short times, shifted relative to the branch relaxation, is dominated by the retraction of branches and backbone end segments. The backbone damping function is rationalized by considering it as a linear chain that feels a smaller effective strain due to the prior branch relaxation.

1. Introduction

In the past decade we have witnessed enormous progress in the understanding of molecular rheology of complex polymers.[1,2] Experimental tests, usually performed in standard shear flow rheometers, can be used to probe molecular architecture effects on the rheological behavior of branched polymers. This will provide the needed ingredients to understand how branching can modify the polymeric flow behavior from that of a simple linear chain. Subtle variations in architecture might not be easily distinguishable in rheological tests so then it is important to understand how the architecture influences different macroscopic properties in order to design polymeric materials with desired properties.[3] In this work we use the comb architecture to investigate the influence of multiple branch points on the stress relaxation behavior of branched polymers.

The comb architecture consists of a linear chain backbone with multiple branches of equal length randomly distributed and attached to the backbone.[4−6] The stress relaxation behavior of comb polymers in the linear (small deformation) regime is well described in the framework of the tube model with the introduction of dynamic tube dilution[7,8] and the concept of a hierarchy of relaxation processes.[9−13] The latter envisions the chain to relax beginning with the outermost branches, using the same mechanism as the arms of a star polymer, and ending with the interior chain segments, which relax like a diluted linear chain.[14] Knowledge of the different linear relaxation mechanisms can be used to determine whether concepts, such as the hierarchy of relaxation processes and dynamic dilution, extend to nonlinear flow situations that are more relevant to the processing performance of such materials.

The step strain experiment is frequently used to study the nonlinear response of polymer systems in the absence of flow. Numerous studies have been performed on linear chains,[15−19] and there is more limited data for star polymers,[1,20−27] H-polymers,[13] pom-poms,[28−31] and more complex architectures.[25,32−40] Previous work on polydisperse branched architectures suggests a rheological response that depends on the macromolecular architecture[33,36,41] because of the presence of the branch points.

The response of more monodisperse comb polymers to nonlinear deformations has been studied recently by Kapnistos et al.[40] and Vega and Milner.[25] Kapnistos et al. presented stress relaxation mastercurves covering the entire relaxation of the comb and demonstrated that the hierarchy of relaxation processes seen in the linear regime still exists under strong nonlinear deformations. Further, both Kapnistos et al. and Vega and Milner utilized the hierarchical relaxation picture to suggest that if the comb backbone remains well-entangled after dynamic dilution due to the arm relaxation process, the backbone should follow the Doi−Edwards[42] prediction for a linear chain, with no dependence on architecture. Each study presents data for combs in solution at different concentrations, and the stress relaxation behavior of the combs seems, qualitatively, to follow the same behavior; as the number of backbone entanglements decreases, the damping function tends toward the dilute linear chain limit. This renders a comparative study of the damping function for a comb backbone

*Corresponding author. E-mail: lgl20@engineering.ucsb.edu.

 Published on Web 11/23/2009

Table 1. Molecular Characteristics of Polyisoprene Comb Polymers

code	$M_{comb} \times 10^{-3}$ [a]	ε_{comb} [b]	$M_{bb} \times 10^{-3}$ [a]	$M_{branch} \times 10^{-3}$ [a]	ε_{branch} [b]	q [c]	T_g [°C]	microstructure (% 3,4-content) [d]	backbone classification
PI132k	132	1.05	85.1	10.2	1.05	4.6	−61	6.2	L
PI159k	159	1.06	137	2.7	1.08	8.2	−61	6.6	H
PI211k	211	1.02	157	6.3	1.02	8.6	−61	6.5	H
PI472k	472	1.04	370	5.8	1.02	17.6	−61	6.2	H

[a] M_x is the weight-average molecular weight of component x, backbone abbreviated as bb. [b] ε_x is the polydispersity index of component x. [c] q is the average number of branches, eq 1. [d] Based upon ^{1}H NMR in $CHCl_3$ at 25 °C.

(with a large number of entanglements after dilution) with the damping function for a linear chain with an equal number of entanglements useful. However, neither paper reports such a comparison. On the other hand, both suggest that at higher entanglement values the comb polymer should follow the linear chain theory of Doi−Edwards, which itself is derived in the high entanglement limit.[42] To check this suggestion, there is clearly a need for data for a comb backbone that remains very well entangled after dynamic and/or static dilution so that entanglement values above those previously studied can be probed. This comb can then be studied in solutions at different concentrations to understand the correlation between the number of entanglements and relaxation.

In the present study, we test comb polymers with short branches and long, well-entangled backbones in linear and nonlinear deformations to further examine the effect of branching on the stress relaxation behavior of the comb backbone. The linear viscoelastic behavior of the short arm combs is used to test the limits of the current theories when the molecular weight of the branches is less than or only slightly larger than the entanglement molecular weight, on the order of 5000 for polyisoprene[43,44] (i.e., $0.5 \leq M_{branch}/M_e \leq 2$), and to explore the relaxation dynamics of comb backbones with multiple branch points that remain well-entangled even after dynamic dilution. The nonlinear experimental data suggest that the deviation of the comb backbone damping functions from the Doi−Edwards linear chain theory is more complex than the current treatment of attributing the response to be solely dependent on the number of backbone entanglements (the method of Kapnistos et al.[40] as well as Vega and Milner[25]). We show that the backbone response is architecture dependent (in the sense that there is a departure from the Doi−Edwards theory even at high entanglement levels), and we present a unified framework to understand the comb stress relaxation data for all of the combinations of materials studied to date.

2. Experimental Procedures and Materials

2.1. Materials. The combs in our present study consist of a long linear backbone to which a moderate number of short branches are attached. The well-defined combs were synthesized by the macromonomer strategy using high-vacuum techniques and the 4-(chlorodimethylsilyl)styrene (CDMSS) linking agent/monomer. Details of the synthesis are given in recent papers.[39,45,46] In brief, the synthesis involved (1) anionic polymerization of isoprene, to give living polyisoprene used for the branches, (2) selective titration of the chlorosilane group of CDMSS with the living polyisoprene to produce a styrenic macromonomer of polyisoprene, and then (3) the anionic copolymerization of the macromonomer with isoprene to produce the final polyisoprene combs. The last step is done in the presence of a randomizer so the branches are assumed to be randomly distributed along the backbone. The average number of branch points (q) is calculated from the weights of the styrenic macromonomer (W_{sMM}) and isoprene (W_{IP}) monomers given that each are transformed almost completely into copolymers[47]

$$q = \frac{W_{sMM} M_{n,comb}}{(W_{sMM} + W_{IP}) M_{n,sMM}} \quad (1)$$

Here $M_{n,sMM}$ and $M_{n,comb}$ are the number-average molecular weights of the macromonomer and comb, respectively. We define the comb to have a linear backbone with backbone molecular weight, M_{bb}, with q branches with branch molecular weight, M_{branch}. The backbone is classified as being lightly (L) or heavily (H) branched using the criteria of Daniels et al.[9] to be explained later. The molecular characteristics of these combs are shown in Table 1.

The overall molecular weight of the comb, M_{comb} and M_{branch}, were characterized by SEC-TALLS (TALLS: two angle laser light scattering) in THF at 35 °C. The polydispersity index of the comb (ε_{comb}) and branches (ε_{branch}) were calculated using SEC in THF at 35 °C. From Table 1, it can be seen that all polyisoprene combs exhibit low polydispersity index(ε) and well-defined characteristics that will enable the analysis of the effect of their architecture on the rheological behavior. We do not consider any polydispersity associated with the number of branches. Throughout the paper, the combs will be referred to by their code, which reflects the overall molecular weight. The polyisoprene combs are perfectly suited to test the hypothesis of Vega and Milner[25] and Kapnistos et al.[40] for the nonlinear response of a well-entangled comb backbone. The architectural features of the combs (number of branches and branch/backbone length) are varied so that the effect of each component can be examined. The short branches of the combs will allow us to probe the relaxation behavior of such short-branch segments and study the effect of the branch point on the relaxation dynamics of a well-entangled backbone. There is a similarity here with the much studied asymmetric star polymers,[43,48,49] as will be discussed below. We study the comb polymers at different concentrations in squalene, nearly an ideal solvent for polyisoprene, to systematically vary the number of backbone entanglements.

The solutions were prepared by dissolving polymer into squalene (Aldrich) at various concentrations using tetrahydrofuran (THF) as a cosolvent. The THF was removed by slow evaporation at room temperature and then at progressively higher vacuum conditions until completely gone. The samples contained small amounts of antioxidant (2,6-di-*tert*-butyl-*p*-cresol) to reduce the risk of degradation during experimental tests. Reproducibility of the measurements serves as the ultimate test of the material's condition. The samples were stored in a freezer and allowed to sit under high vacuum for 24 h before testing to remove any possible moisture.

2.2. Rheological Measurements. The linear and nonlinear rheological tests were carried out using two Rheometrics Scientific controlled strain rheometers of low (ARES-2kFRT) and high-resolution ranges (ARES-100FRT) at controlled temperatures. Rheological tests on the low resolution instrument were run at temperatures from −60 to 70 °C via an air/nitrogen convection oven with a liquid nitrogen Dewar. The temperature of the high-resolution rheometer is controlled with a fluid bath that had a more limited temperature range (5−70 °C). A wide combination of available and custom-made cone and plate geometries were used on the two rheometers to overcome many of the instrumental limitations (compliance, torque, etc.) and obtain reliable results.[40,50] For linear viscoelastic tests parallel plates of diameter 7.9 or 25 mm were chosen. Samples with long relaxation times (melts) were press-molded under vacuum into disks for ease of loading into the rheometer and to eliminate air bubbles in the sample. Prior to tests, the polymer was

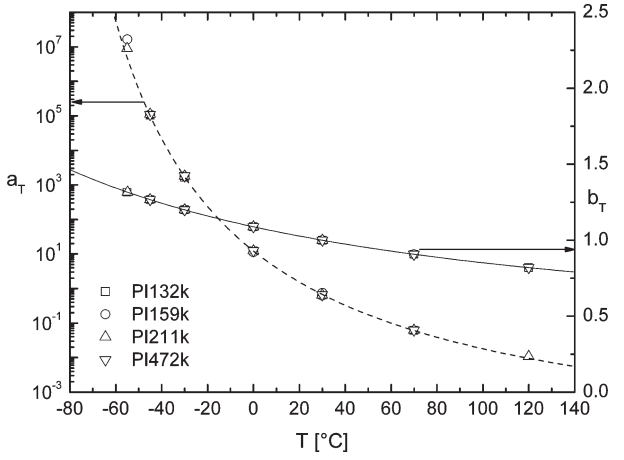

Figure 1. Horizontal (a_T) and vertical (b_T) shift factors for polyisoprene comb melts PI132k (□), PI159k (○), PI211k (△), and PI472k (▽) at reference temperature T_{ref} = 25 °C. Symbols represent parameter values used to create master curve. Solid line (—) indicates vertical shift function, and dashed line (---) is WLF function with C_1 = 4.5, C_2 = 132 °C, and T_{ref} = 25 °C.

equilibrated at the test temperature, and care was taken to ensure that residual stress due to loading was relaxed. Strain sweeps were conducted to verify that frequency sweeps were performed in the linear viscoelastic regime.

Because of the limited frequency range of the rheometers, rheological tests for each sample were run at multiple temperatures to probe different relaxation processes. Low-temperature experiments were performed to probe the faster relaxation processes of the polymer, in this case enabling us to view the relaxation of the short comb branches. Mastercurves capturing the linear viscoelastic behavior of the comb polymer from branch to backbone relaxation were created using the time−temperature superposition (tts) principle.[51] The data were shifted vertically to account for the change of density with temperature

$$b_T = \frac{\rho(T_{ref})(T_{ref} + 273.15)}{\rho(T)(T + 273.15)} \quad (2)$$

where the temperature is in °C. The density dependence for polyisoprene was calculated by fitting a straight line to experimental data from Zoller and Walsh:[52] $\rho(T) = 0.9227 - 5.907 \times 10^{-4}T$ (ρ in g/cm^3, T in °C). The horizontal shift factors for the polymer melts were fitted using a single set of parameters (T_{ref} = 25 °C, C_1 = 4.5, C_2 = 132 °C) for the WLF function:

$$\log(a_T) = \frac{-C_1(T - T_{ref})}{C_2 + T - T_{ref}} \quad (3)$$

These shift factors compare well with reported values for linear[53,54] and star polyisoprene.[43] The samples exhibit the same shift factors (Figure 1) for the nonlinear and linear tests, which permits the creation of mastercurves to view the relaxation behavior across large time scales.

The nonlinear step strain experiments were performed at multiple temperatures to probe the response of different relaxation processes to the deformation. There are technical issues that need to be addressed when performing nonlinear step strain experiments that have been discussed in detail by previous works.[40,50,55,56] We followed the methodology detailed by Kapnistos and co-workers[40] for the experimental procedure. A physical limitation of the experimental setup is the strain imposition time of the ARES step motor, which can influence the stress relaxation behavior of the polymer.[55] If the imposition time were longer than the relevant Rouse time (branch or backbone) or even if greater than the longest relaxation time, one would then need to assume the chain to have partially retracted before the imposition of stretch was complete.

For the imposition of strain at low temperatures, $\tau_{R,branch}$ is the relevant Rouse time. As the strain increases, the time needed for the motor to reach the commanded strain typically lengthens (Figure 2a), especially at low temperatures or for high concentrations or melts. In Figure 2a the imposition time of the motor is close to the relaxation time of an entanglement segment, τ_e, and shorter than all characteristic relaxation times of the branches ($\tau_{R,branch}$, τ_{branch}) and backbone ($\tau_{R,bb}$, τ_d). Here the Rouse time of the backbone, $\tau_{R,bb}$, is calculated from the friction of the branch points, and τ_d is the reptation time of the backbone. At this temperature the deformation is then an ideal step strain for the branches and backbone.[21,55] If this sample is tested at higher temperatures (Figure 2b), the imposition time of the motor is now slower than $\tau_{R,branch}$ but still quicker than τ_{branch}, $\tau_{R,bb}$, and τ_d. The validity of tts for the nonlinear stress relaxation data is shown in Figure 2c with the relaxation data at −60 °C (Figure 2a) shifted to −40 °C (Figure 2b). The stress relaxation mastercurve is shown in Figure 2d. The stress relaxation mastercurves can be considered as measurements at the reference temperature. The strain history that is important is the motor imposition time at the lowest temperature used to create the mastercurves. The strain imposition times of the motor were found to be shorter than $\tau_{R,bb}$ so that we could expect that the backbone was not retracting before the complete imposition of strain.

Between step strain experiments a waiting time longer than 10 times the longest relaxation time of the polymer was applied to ensure complete relaxation of the comb. For tests at low temperatures (e.g., −60 °C) where the waiting time for complete relaxation would be quite long, the sample was heated up to a temperature where the longest relaxation time was reasonably attainable. The step deformations at low temperatures allowed us to study the behavior of the comb branches under strong deformation and then analyze the effect of the branch points on the stress relaxation behavior of the backbone on longer time scales (higher temperatures). After nonlinear experiments, the linear viscoelastic behavior was checked to verify sample adhesion to the plates[18] and test for degradation. Stress relaxation mastercurves were created using time−temperature superposition;[40,41] with each shift factor compared against values used in the linear viscoelastic tests to help validate the data. We used the vertical shift factors to discern the presence of slip in the nonlinear tests, as slip would greatly increase the shift needed to create the mastercurve.[40]

3. Theoretical Framework for Data Analysis

3.1. Linear Viscoelastic Response. The linear relaxation of comb polymers with well-entangled branches and backbone is well understood in the framework of the tube model with the introduction of dynamic tube dilation and the concept of a hierarchy of processes that allow the chain to relax, beginning with the branches and free backbone chain ends and ending with the relaxation of the interior chain segments.[7,10] The anzatz known as dynamic tube dilution was first introduced for linear melts by Marrucci[8] and for star polymers by Ball and McLeish.[7] The idea behind dynamic dilution is that as the polymer segments relax, they effectively act as a solvent for the rest of the polymer since they will no longer hold entanglements. As the segments of the polymer relax, the entanglement network becomes increasingly diluted and the diameter of the polymers' confining tube increases. For comb polymers, hierarchical relaxation dictates that the branches and backbone ends relax first and then due to dynamic dilution, the remaining backbone relaxes like a linear chain in a solution (with entanglements between backbones only). The linear viscoelastic relaxation

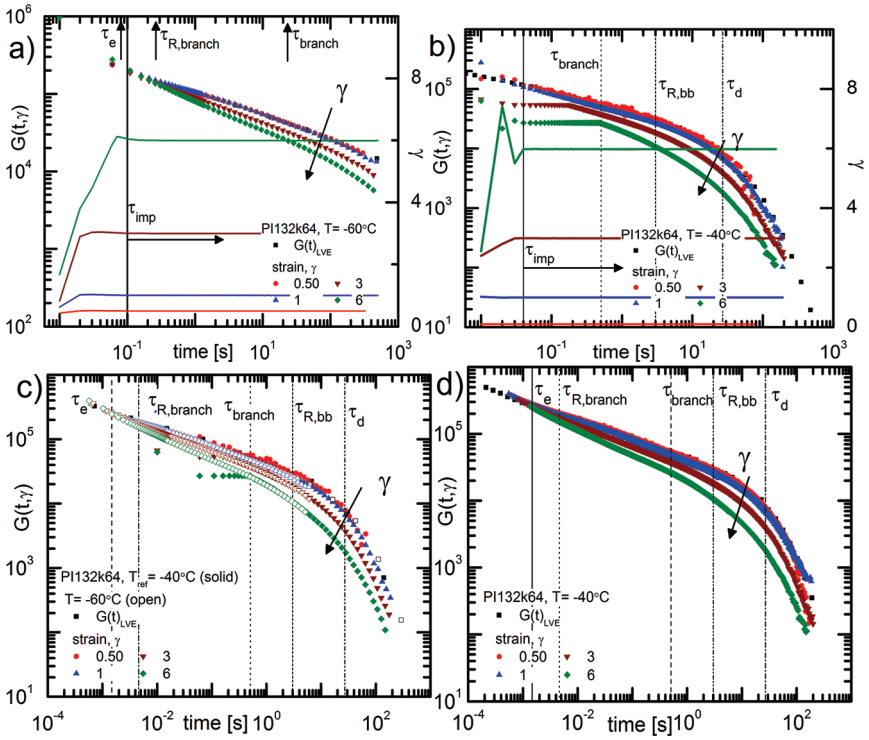

Figure 2. Nonlinear step shear strain measurement of PI132k in squalene at 64% compared with $G_{LVE}(t)$ (■). The deformation profile is drawn with solid lines (—) and the relaxation modulus with symbols (●). Time scales from linear viscoelastic relaxation are marked with dashed lines, and for (a) and (b) τ_{imp} marks the time scale after which data is considered due to imposition of a steady strain. (a) Test at $T = -60$ °C to probe short time relaxation of comb. Imposition time of motor is less than Rouse time of branch and backbone, $\tau_{imp} < \tau_{R,branch} \ll \tau_{R,bb}$. (b) Test at $T = -40$ °C to probe relaxation of backbone. Imposition time of motor is greater than $\tau_{R,branch}$ but less than τ_{branch} and $\tau_{R,bb}$. $\tau_{R,branch} < \tau_{imp} \ll \tau_{branch} < \tau_{bb}$. (c) tts of data from $T = -60$ °C (□) to $T_{ref} = -40$ °C (■). (d) Mastercurve of stress relaxation created at $T = -40$ °C.

mechanisms resemble a star at shorter time scales when the branches and backbone ends are relaxing and a linear chain during backbone relaxation. The backbone relaxes like a linear chain with heavy friction blobs at the branch points that impede the mobility of the chain.

We will model the linear viscoelastic behavior of the short arm polyisoprene combs via a tube-model theory using the work of Kapnistos et al.,[11] who succeeded in fitting the rheological behavior of highly entangled polybutadiene and polystyrene linear combs. The details and derivations of the theoretical model describing the relaxation of the comb polymer are beyond the scope of this paper and can be found elsewhere.[11,50] The relaxation of the comb occurs in sequential steps according to the hierarchical relaxation hypothesis, which are all accounted for in the model.

1. At times less than the Rouse time of an entanglement segment, τ_e, the backbone and branches undergo free Rouse motion unconstrained by surrounding chains.

2. On time scales longer than τ_e the segments feel constraints due to the surrounding chains and the concept of a tube becomes relevant, prohibiting transverse motion. Branches and backbone segments at backbone ends, $M_{bb,end} = M_{bb}/(q+1)$, begin relaxing stress through fluctuations identical to the arm motions of a star polymer (see Kapnistos et al.[11] for full description of comb ends). Backbone segments that lay between branch points are inhibited from free motion due to immobility of branch points on these time scales.[9−13]

3. The branches relax on a time scale, τ_{branch}, releasing entanglement constraints between branches and backbones, giving rise to the so-called dynamic dilution (see step 4 below).

4. The backbone remains entangled with other backbones and relaxes like a diluted linear chain with friction blobs at the branch points. The branches fluctuate on time scales of τ_{branch}, and it is assumed that backbone segments can only move to explore new configurations when a branch retracts/fluctuates back to a branch point. This greatly impedes the time scale for relaxation of the "linear chain" backbone. Initially, the backbone relaxes stress by retracting, i.e., relaxing stretch, within the tube, and then explores new configurations, via "chain length fluctuations" equivalent to a two-arm star,[11,57] where the time scale for these fluctuations is dependent upon the time scale for branch retraction. Short fluctuations into the tube are unaffected by the entropic potential and the ends of the backbone chain diffuse freely through Rouse motion in the tube.[43] These motions are called early time scale fluctuations, τ_{early}. As the fluctuations become deeper, the entropic potential becomes important and the expected relaxation time of a chain segment is calculated using an activated process, τ_{late}.[58]

5. The comb backbone can eventually relax stress faster via reptation as the backbone diffuses longitudinally out of the constraining tube under dynamic dilution. This relaxation mechanism relaxes the remaining stress on time scales τ_d.

The derivation of the backbone early time, τ_{early}, depends on the level of branching, and the early fluctuation time for lightly branched combs was calculated assuming that each branch point moved independently. The backbone motion in heavily branched systems was modeled as a Rouse chain with a bead at each branch point, distributing the drag over the entire backbone. Daniels et al.[9] introduced a criterion to determine if a comb were to be classified as lightly or heavily branched that depended on the number of branch points in

the backbone segment that relaxed by fluctuations. A backbone is heavily branched if

$$q > \left(\frac{2M_{bb}}{M_e(\phi_{bb}(1-x_d))^{-1}} \right) \tag{4}$$

where x_d is the dimensionless distance along the backbone where reptation takes over. The lightly (L) or heavily (H) branched classification of the polyisoprene combs was given in Table 1, and the corresponding equation for τ_{early} was used in the linear viscoelastic model.

We recognize that there are limitations in applying the Kapnistos et al.[11] tube model, derived for entangled systems, to our comb polymers with weakly entangled branches. Since the model was not designed to specifically handle the transition between unentangled and entangled dynamics, we apply it with the intention of obtaining an understanding of the short branch relaxation. The use of this model for the weakly entangled branches assumes that the short branches employ the same relaxation mechanisms as an entangled branch to relax stress.

The Kapnistos et al. model contains parameters that are either known, taken from linear viscoelastic data or used as fit parameters. The comb characteristics (Table 1) are used for parameters such as the number of branches or branch and backbone molecular weights. The plateau modulus, G_N, is evaluated from linear viscoelastic data as $G'(\omega)$ at the intermediate frequency minimum in $\tan(\delta)$. The details and actual values will be given in the next section along with the experimental data. We then calculate the entanglement molecular weight using Ferry's definition[51]

$$M_e = \frac{\rho(T)RT}{G_N(T)} \tag{5}$$

The number of entanglements, Z, are calculated with the standard relationships[59]

$$Z_{branch} = \frac{M_{branch}}{M_e}\phi_p^{\alpha_S} \tag{6}$$

and

$$Z_{bb} = \frac{M_{bb}}{M_e}\phi_p^{\alpha_S}\phi_{bb}^{\alpha_D} \tag{7}$$

where ϕ_p is the volume fraction of polymer and the volume fraction of polymer that is backbone is calculated using the relationship

$$\phi_{bb} = \frac{M_{bb}}{M_{bb} + qM_{branch}} \tag{8}$$

The value of the dilution parameter, α, for both static (S) and dynamic (D) dilution in eqs 6 and 7 remains an unsettled issue in the literature, though it is generally agreed that the value is between 1 and 4/3.[1,2,7−9,59−62] We will compare the theoretical model with experimental data to determine the value of α. The Rouse time of an entanglement segment, τ_e, is chosen so that the theoretical predictions fit the experimental data at high frequencies.

The friction parameter p^2 is related to the fraction of the tube radius that the branch point can move after each branch retraction. A value of $p^2 = 1/12$ has been used successfully to model the linear viscoelastic data of polybutadiene and polystyrene combs[11,12] and polyisoprene H-polymers.[13] Other authors have proposed that p^2 be chosen to represent the frictional resistance each branch point experiences[39,49,63,64] or varied the value to match experimental data.[43] A time marching algorithm developed by van Ruymbeke et al.[65] eliminates the parameter with $p^2 = 1$ to successfully model the behavior of asymmetric stars, H-polymers, pom-poms, and dendritic structures. However, whereas this is a tube-model theory with the same physics, the various relaxation modes are introduced differently, and moreover it has not been applied yet to combs. Here, we will proceed with the Kapnistos et al. approach and use the value $p^2 = 1/12$.

3.2. Theory To Describe Nonlinear Step Strain Flow. Unlike the linear viscoelastic regime, where the relaxation modulus $G(t)$ is independent of the strength of deformation, the nonlinear relaxation modulus is strain dependent, $G(t,\gamma)$. In nonlinear deformations, the stress relaxation of the polymer (i.e., dominant relaxation mechanisms) can vary depending on the strength of the flow. For many polymer systems, the stress relaxation curves after a step deformation exhibit time−strain separability so that after a characteristic time, τ_k, the relaxation of the chain is dominated by relaxation mechanisms that are independent of the strain, and the curves can be vertically superposed. For linear chains the time scale τ_k typically resides between τ_R and τ_d. As a result of the superposition, the nonlinear response can be decomposed as the linear viscoelastic response, $G(t)$, multiplied by a strain-dependent function, $h(\gamma)$, called the damping function.[19,66,67]

$$G(t,\gamma) = h(\gamma)G(t) \tag{9}$$

The damping function is the vertical shift required to superpose the stress relaxation curves for a given initial strain γ. The results of nonlinear step strain flows are typically analyzed in terms of $h(\gamma)$, which is the fraction of initial stress that is not relaxed before the linear relaxation mechanisms dominate the chain dynamics.[68]

The tube theory of Doi and Edwards[42] correctly predicts the response of entangled linear chains to a step deformation. The theory is derived at the high entanglement limit and assumes that the confining tube is instantaneously deformed and that the primitive chain is stretched from its original length, L_0, to a length $\lambda(\gamma)L_0$. Using the notation of Doi and Edwards, $\lambda(\gamma)$ is the chain stretch averaged over all possible chain segment orientations

$$\lambda(\gamma) = \langle|\mathbf{E}\cdot\mathbf{u}_0|\rangle_0 \tag{10}$$

Here $\mathbf{E}$ is the deformation gradient for a shear deformation, and $\langle\ldots\rangle_0$ denotes an average over an isotropic distribution of unit vectors, $\mathbf{u}_0$. The chain retracts back to an equilibrium length on the Rouse time scale, τ_R, vacating a portion of the tube, which corresponds to a reduction in the modulus.[69] After the retraction process a majority of the remaining stress is relaxed through reptation on time scales, τ_d. We note that the Doi−Edwards theory assumes a constant tube diameter throughout the processes of deformation and retraction (although theories based on different constraints have been proposed by several researchers[41,67,70]). The damping function predicted by Doi and Edwards[42] is

$$h(\gamma) = \frac{\mathbf{Q}^{DE}(\gamma)}{\mathbf{Q}^{DE}(\gamma')_{\gamma'\to 0}} \tag{11}$$

where the strain measure tensor is given by

$$\mathbf{Q}_{DE}(\gamma) = \frac{1}{\langle|\mathbf{E}\cdot\mathbf{u}_0|\rangle_0}\left\langle\frac{\mathbf{E}\cdot\mathbf{u}_0\mathbf{E}\cdot\mathbf{u}_0}{|\mathbf{E}\cdot\mathbf{u}_0|}\right\rangle_0 \tag{12}$$

Without independent alignment, the damping function is often approximated by the function[40,42,67,71]

$$h(\gamma) = \frac{1}{1 + \frac{4}{15}\gamma^2} \quad (13)$$

which has a value of 1 at low strains (linear regime). The Doi−Edwards prediction for $h(\gamma)$ has also been shown to be applicable for star polymers.[24] The previous work on comb polymers by Kapnistos et al.[40] extended the time range of the damping function (via tts) and demonstrated that hierarchical relaxation exists in the nonlinear step strain flow, which enables one to calculate the damping behavior of both the branches and the backbone.

On time scales relevant to the branch relaxation (referring to the linear response), the comb can be viewed as having two types of segments: backbone segments between branch points that are unable to retract, and branches and the free ends of the backbone that can both retract. The polymer stress is calculated by summation of the individual stress contributions of each segment (i.e., both retracted and stretched). This idea was originally proposed by Bick and McLeish[34] to develop a damping function for polymer molecules with different architectures including comb polymers and adopted by Kapnistos et al.[40] to examine the damping behavior of combs with well-entangled branches. The original theory of Bick and McLeish included a branch point withdrawal mechanism, which assumed that if the forces on the backbone due to the deformation passed a critical threshold, the backbone segment would pull the branch point into the tube, hence relaxing stress. Because of the short lengths of the branches analyzed in this study, the effect of branch point withdrawal is hard to distinguish in the deformation range available (without slip). Without branch point withdrawal, the short time damping function corresponding to the branch and free end relaxation is calculated by Kapnistos et al. as

$$h_{\text{branch}}(\gamma) = \frac{[(1-\phi_{\text{retract}})\alpha(\gamma)^2 + \phi_{\text{retract}}]\mathbf{Q}^{\text{DE}}(\gamma)}{\frac{4}{15}\gamma} \quad (14)$$

where ϕ_{retract} is the fraction of the comb that is free to retract on the branch time scale. It can be seen from (14) that this short time damping function for the comb will have a weaker dependence on strain than expected via the Doi−Edwards theory for a linear chain because of the stretched backbone segments that only relax on longer time scales. We will refer to damping behavior that exhibits a weaker dependence on strain, relative to the Doi−Edwards theory, as softer damping. The extent to which the damping behavior of the comb changes between the branch and backbone relaxation time scales will of course depend on the value of ϕ_{retract}.

The response of the backbone to the step deformation is probed by shifting the stress relaxation curves on time scales relevant to the backbone relaxation. Recent work has hypothesized that it should be possible to model the backbone damping behavior via the Doi−Edwards theory for linear chains if the backbone is heavily entangled. Vega and Milner[25] examined a single polyethylene comb polymer at different dilution values and found damping behavior that was dependent on the number of backbone entanglements and appeared to be tending toward that of a dilute linear chain as the number of entanglements is decreased. We believe that it is noteworthy that their data are never equivalent to the Doi−Edwards theory, although they suggest that it would be if the backbone were studied in a more entangled state (more than 20 entanglements, based upon a dilution parameter of 1 to be consistent with our calculations). It is worth pointing out, however, that linear chains and stars show agreement with the Doi−Edwards theory at much lower entanglement levels: $Z_{\text{linear}} = 4$[56] and $Z_{\text{star}} = 2$.[23] While Vega and Milner presented data for a single polyethylene comb at different concentrations, the recent work of Kapnistos et al.[40] presents data for five different polybutadiene and polystyrene combs in solution with postdilution backbone entanglement values ranging from 1 to 5 (using a dilution parameter of 1). The data of Kapnistos et al. are qualitatively similar to that of Vega and Milner, with comb backbones exhibiting softer damping behavior as the number of backbone entanglements (after static and dynamic dilution) is decreased. Kapnistos et al. also presented slip spring simulations of linear chains that matched the experimentally observed damping behavior of their comb backbones when the number of entanglements was equal to the number of entanglements estimated for the backbone after dynamic dilution. From these two most recent studies, it would appear that the moderate number of backbone entanglements, after dynamic dilution, is the sole cause of the "softening" of the damping function for comb polymers away from the Doi−Edwards theory. Therefore one would expect the well-entangled backbones of the polyisoprene combs that are studied in this paper to follow the Doi−Edwards curve.

4. Results and Discussion

4.1. Linear Viscoelastic Behavior. The linear viscoelastic behavior of the comb polymers is used to determine the influence of short branches on the stress relaxation behavior. The short length of the branches will allow us to make analogies to the behavior of short star arms, and the well-entangled backbones will permit us to distinguish the effect of the branch points on the backbone dynamics from the effects of small numbers of entanglements. The combs were examined in the melt and at different concentrations in squalene, and the linear viscoelastic mastercurves are presented in Figure 3.

The hierarchical relaxation of the comb architecture implies that there will be distinct relaxation modes at intermediate and low frequencies corresponding to the branches and backbone, respectively. In general, the intermediate frequency plateau is a consequence of the branch relaxation, during which the backbone is essentially frozen due to the presence of the branch points. Lightly entangled chains do not show a plateau modulus, so we do not expect to see an intermediate frequency plateau for the lightly entangled branches, but we do expect a low frequency plateau for the highly entangled comb backbones. Because the plateau modulus is not always apparent for the polymer chains, the data are also presented in the form of the tangent of the phase angle ($\tan(\delta) = G'/G''$), which is more sensitive in distinguishing features of the relaxation processes and can be used to differentiate the relaxation modes of the short branches.[11] Referring to Figure 3e, PI159k (b), PI211k (c), and PI472k (d) exhibit a distinct low-frequency minimum in $\tan(\delta)$ associated with the backbone relaxation. The minimum (solid ↑) or inflection (open ↑) in $\tan(\delta)$ is marked for the branch (down) and backbone (up), respectively. The minimum is calculated from the lowest value of $\tan(\delta)$, and the inflection is measured from the change in slope of $G''(\omega)$. The relaxation of the branches releases constraints on the backbone effectively dilating the backbone tube, which is evident through a reduced value of the relevant plateau modulus that scales as

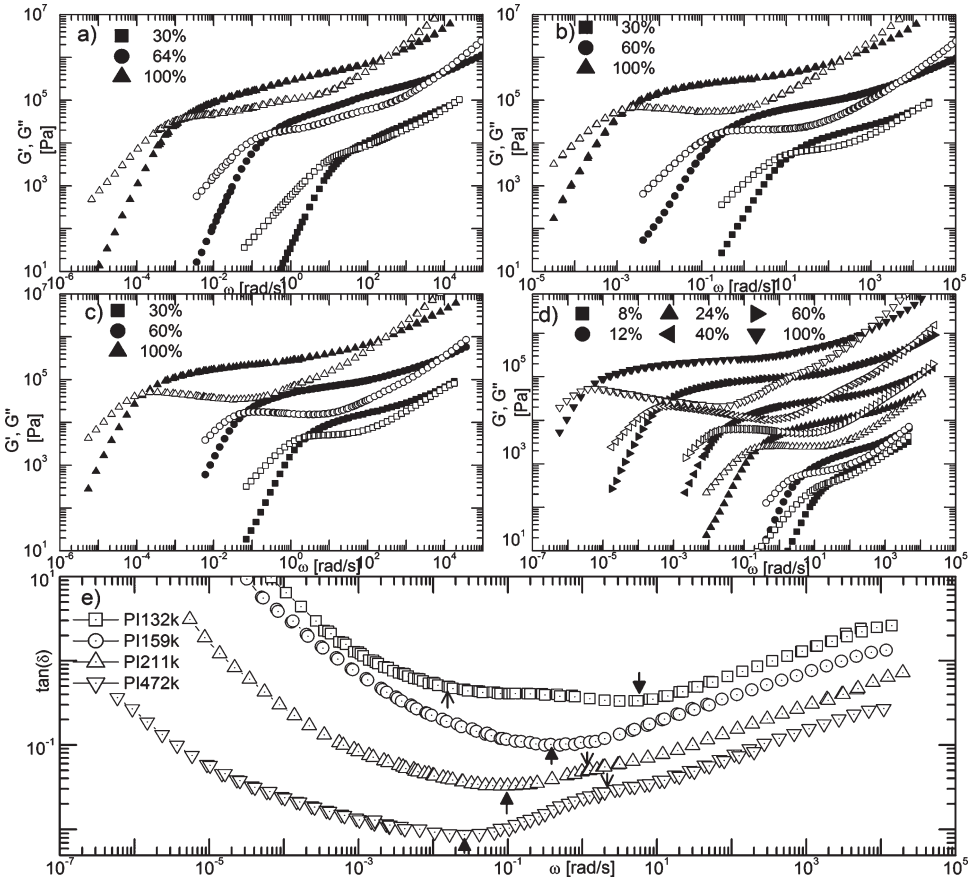

Figure 3. Linear viscoelastic frequency spectra (G', closed symbol; G'', open symbol) for polyisoprene comb polymers at −30 °C: (a) PI132k ϕ = 0.3 (■), ϕ = 0.64 (●), and ϕ = 1 (▲). (b) PI159k ϕ = 0.3 (■), ϕ = 0.6 (●), and ϕ = 1 (▲). (c) PI211k ϕ = 0.3 (■), ϕ = 0.6 (●), and ϕ = 1 (▲). (d) Selected curves for PI472k ϕ = 0.08 (■), ϕ = 0.12 (●), ϕ = 0.24 (▲), ϕ = 0.40 (right-pointing ▲), ϕ = 0.60 (left-pointing ▲), and ϕ = 1 (▼). (e) tan(δ) = G'/G'' for the comb melts: PI132k (⊡), PI159k (⊙), PI211k (△), and PI472k (dotted ▽) multiplied by 1, 0.5, 0.2, and 0.1, respectively, for clarity of presentation. The minimum (solid ↑) or inflection (open ↑) in tan(δ) is marked for the branch (down) and backbone (up), respectively.

$\phi_{bb}^{\alpha+1}$.[62] The backbone relaxation of PI132k (Figure 3a) is less entangled and marked by an inflection in tan(δ) (Figure 3e). The intermediate frequency relaxation of the branches is most apparent for PI132k, which has a distinct intermediate frequency minimum in tan(δ) (Figure 3e). The rubbery plateau modulus, G_N = 0.4 MPa evaluated as $G'(\omega)$ at the intermediate frequency minimum in tan(δ), was used to calculate the entanglement molecular weight using eq 5. The calculated value, M_e = 4730, is within 10% reported values for polyisoprene.[39,43,44] As the number of branch entanglements is decreased, the branch relaxation is represented by an inflection in tan(δ) (e.g., PI211k, $Z_{branch} \sim 1.3$ and PI472k, $Z_{branch} \sim 1.2$), and below one entanglement there is no apparent effect on tan(δ) (e.g., PI159k, $Z_{branch} \sim 0.5$).

In the framework of dynamic tube dilution, the relaxation time of an unentangled branch is so short that we should expect it to essentially act as a solvent for the backbone instead of delaying the relaxation through the hierarchical process. In this case, the backbone should be expected to resemble a linear chain in solution. Work by van Ruymbeke et al.[72] on pom-poms with unentangled branches indicated that the relaxation behavior could be modeled by a blend of linear chains with the short chains being the length of the unentangled branch. The molecular weight (to account for the extra friction of the branch) of the long chain was equal to the backbone molecular weight (for the pom-pom this is the chain between the two branch points) plus the molecular weight of two branches. For our case, this is equivalent to making the long component in the blend equal to the longest possible linear chain in the architecture that is consistent with the our view of the comb architecture and treatment of the backbone ends.[11] The polyisoprene combs have backbone ends that are longer than the branches so in each case the backbone is the longest linear chain in the architecture.

In order to test the expectation that a comb with branches shorter than M_e will act like a linear chain with the branches simply playing the role of a solvent, we compare the measured relaxation behavior of PI159k with theoretical predictions for a linear blend. The backbone is treated as a long linear chain with molecular weight equal to M_{bb} and volume fraction ϕ_{bb}, and the short unentangled branches are assumed to act as a solvent. The relaxation of the linear chain was predicted using the quantitative theory of Likhtman and McLeish[73] with τ_e, Z, and G_e calculated using characteristic values for polyisoprene diluted at ϕ_{bb}.

The theoretical predictions are shown by the dashed lines in Figure 4, together with the experimental data. The comparison made utilizes a dilution parameter of 1, the value used previously for the static dilution of comb polymers.[11] A further rationalization of this choice will be shown in the next section. It can be seen that the measured terminal time of the comb is substantially longer than the prediction for the linear chain, which indicates that the short branches act as more than a solvent to the backbone. Another way of visualizing the effect of the branches on the intermediate frequency relaxation of the comb can be obtained by shifting (increasing) τ_e of the linear chain model to match the terminal behavior of the comb backbone. The result is shown by the

solid lines in Figure 4. This highlights the difference between the linear chain and the comb in the intermediate frequency portion of the linear viscoelastic curve where the relaxation of the branches occurs. The low-frequency plateau modulus of the comb is the same as the linear chain, which implies that the dilution of the backbone due to the short chains is consistent with our expectations. Although the branches are apparently unentangled for this PI159k system, it is clear that they still delay (hierarchical relaxation) and dilute (dynamic dilution) the comb backbone in-line with our qualitative expectations for an entangled comb architecture. To corroborate and quantify this "expectation", we need to compare the relaxation behavior with a model that incorporates hierarchical relaxation.

We thus use the linear viscoelastic theory for combs from the work of Kapnistos et al.[11] in order to see whether it can predict the relaxation of the polyisoprene combs with short branches. Although the theory was developed for well-entangled branches, we shall see that it provides useful insights into the relaxation behavior of combs with lightly entangled branches. We compare the model predictions with experimental data to determine the values of τ_e and the static and dynamic dilution parameters.

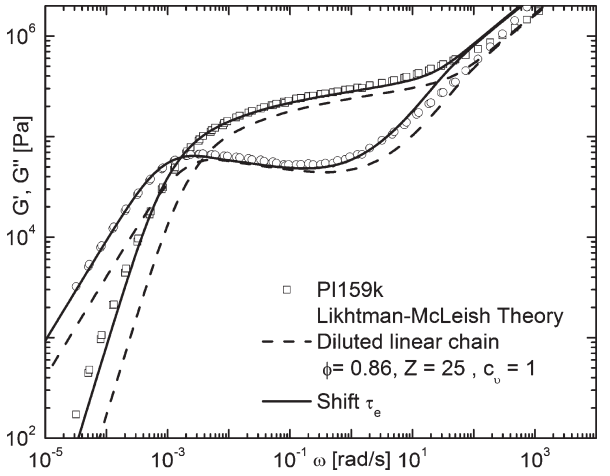

Figure 4. Linear viscoelastic spectrum for polyisoprene comb PI159k (□, ○) compared with a linear chain predicted using the Likhtman and McLeish theory.[73] The linear chain entanglement and dilution are equal to the comb backbone with branches acting solely as a solvent. Predictions are shown for the linear chain relaxation with characteristic parameters for polyisoprene (---) and with τ_e shifted to match low-frequency backbone reptation (—).

We begin by using the relaxation behavior of the comb melt to determine the value of α_D. The relaxation behavior of the PI132k melt is compared against predictions of the Kapnistos et al. theory with characteristics from Table 1 and $p^2 = 1/12$ for $\alpha_D = 1$ (—) and 4/3 (---) in Figure 5a. The value of $\tau_e = 7.9$ ms was chosen to match the high frequency relaxation of the combs at $T = -30$ °C. As a check we calculate the friction coefficient, ζ, at $T = 298$ K using τ_e and the shift factors in Figure 1 with the equation[74]

$$\zeta = \frac{3\pi^2 k_B T}{\frac{M_e^2}{M_0}\frac{\langle R_0^2\rangle}{M}}\tau_e \qquad (15)$$

Here M_0 is the monomer molecular weight and $\langle R_0^2\rangle/M = 0.596$ Å^2 mol/g is taken from Fetters.[75] For the polyisoprene combs considered here, $\zeta = 3.89 \times 10^{-10}$ N s/m, which is in good agreement with values reported in the literature.[76] An input value of $G_N = 0.66$ MPa is required for the model to predict the experimental value, $G_N = 0.4$ MPa, evaluated as $G'(\omega)$ at the intermediate frequency minimum in tan(δ), due to the Z dependence of the plateau modulus in the model that will be discussed below.

It is evident from Figure 5a that the model with $\alpha_D = 4/3$ underpredicts both the terminal time of the backbone and the effect of branch dilution on the backbone plateau modulus. On the other hand, the predictions with $\alpha_D = 1$ capture the relaxation of the backbone and will be used for subsequent calculations. We emphasize that the comparison in Figure 5a does not prove that the dynamic dilution parameter for our comb polymers should be $\alpha_D = 1$. It simply shows that the best comparison between the data and the Kapnistos model is achieved using this value. We next determine the static dilution scaling parameter α_S by comparison of the model predictions with data for solutions of the PI132k comb.

In Figure 5b,c we compare experimental data for PI132k at 64% and 30% in squalene with model predictions using different values for α_S and α_D. It is apparent from the theoretical predictions that a value of 1 for both static and dynamic scalings gives the best predictions of the relaxation behavior of the entire comb, from branch to backbone relaxation. Increasing the static dilution parameter to $\alpha_S = 4/3$ lowers the expected number of entanglements and the backbone terminal time is predicted to be much quicker than is experimentally observed. The predictions in Figure 5a−c demonstrate that the model captures the entire relaxation of the combs with $\alpha_D = 1$ and $\alpha_S = 1$. Again, we do not suggest that these comparisons provide theoretical justification for these values.

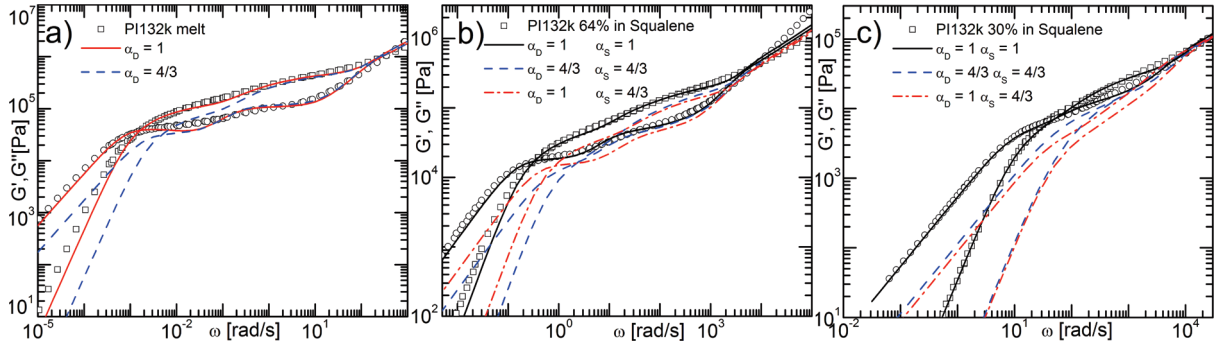

Figure 5. Linear viscoelastic relaxation of polyisoprene comb PI132k compared with theoretical predictions of Kapnistos et al. theory with molecular characteristics and $p^2 = 1/12$ for different values of the dilution parameter (a) melt with predictions for $\alpha_D = 1$ (—) and $\alpha_D = 4/3$ (---), (b) 64% polymer in squalene with $\alpha_D = 1$, $\alpha_S = 1$ (—), $\alpha_D = 4/3$, $\alpha_S = 4/3$ (---), and $\alpha_D = 1$, $\alpha_S = 4/3$ (-·-), and (c) 30% polymer in squalene with $\alpha_D = 1$, $\alpha_S = 1$ (—), $\alpha_D = 4/3$, $\alpha_S = 4/3$ (---), and $\alpha_D = 1$, $\alpha_S = 4/3$ (-·-).

The arguments of the preceding paragraphs for choosing α focused on the model prediction of relaxation time scales. However, also inherent in Figure 5 is the scaling of G_N. Ultimately, the low entanglement levels of the comb branches and the corresponding lack of an intermediate frequency plateau for most of the combs does not allow an examination of the scaling of G_N with ϕ based solely on experimental data. It is clear from Figure 5 that the model with α = 1 most accurately predicts the scaling of the branch and backbone moduli due to static and dynamic dilution. The predictions are made with G_N from the fit of the model to the melt experimental data. From here on we will refer to the dilution parameter as α for both static and dynamic dilution. We notice that Kapnistos and co-workers[11,62] have used α = 1 to fit well-entangled combs with linear and star backbones. The number of branch and backbone entanglements for the various combs and their solutions, calculated using eqs 6 and 7, are shown in Table 2.

A few additional comments are, perhaps, warranted in the view of the unresolved controversy over the theoretically "correct" value of the dilution parameter. A further complication in the analysis of the plateau modulus is the fact that tube models are known to have a dependence of the plateau modulus with Z.[73,77,78] In the Kapnistos et al. model this dependence is evident for combs with $Z_{branch} < 50$. An important and expected property of the model is that the scaling of the low-frequency estimate of the modulus based upon the maximum of G' at low frequency is the same as the scaling of G at the intermediate frequency minimum of tan(δ). A further property of the model that we had not previously noted is that both of these quantities scale relative to $G_N(1)$ as $\phi^{2.1}$ provided that the diluted entanglement levels of the backbone exceed $Z = 15$, with lower values closer to ϕ^2 for lower values of Z. The fact that the predicted scaling of the terminal modulus is not weaker than that of the plateau modulus, and the overall quality of the predictions suggest that our self-consistent approach gives predictions in the right direction. However, clearly more work is needed to elucidate the dilution parameter for branched polymers, but this is beyond the scope of the present contribution.

The relaxation behavior of each comb is predicted using the molecular characteristics in Table 1 and the parameter values α = 1 and $p^2 = 1/12$ in the Kapnistos et al. theory. The results are plotted and compared with the experimental data in Figure 6.

The ability of the Kapnistos theory, implemented in this way, to predict the comb relaxation behavior clearly varies based on the number of branch entanglements. For the comb with the most entangled branches, PI132k, the branch and backbone time scales predicted by the model agree well with the experimental data. The difference between the model predictions using a lightly or heavily branched derivation[9,11,12] of τ_{early} is demonstrated in Figure 6a for PI132k, the only comb which fit the criteria as a lightly entangled backbone (Table 1). The ability to match the model predictions at high frequencies to the experimental data with τ_e and then predict the key features of PI132k relaxation using the characteristics of the comb from Table 1 confirms that the model is robust and captures the correct physics.

As we examine the theoretical fits of the other combs, with lower branch entanglement levels compared to PI132k, we find that the model fails progressively to capture the relaxation behavior. This is most apparent in the relaxation behavior of PI159k, where the model fails to describe the relaxation of the unentangled branches, and as a result the relaxation of the backbone is also misrepresented. But the backbone is also predicted to relax too soon for combs

Table 2. Polyisoprene Comb Solutions Studied[a]

sample	ϕ_p	$\phi_p\phi_{bb}$	Z_{branch}	Z_{bb}
PI132k	1.00	0.65	2.2	11.6
	0.64	0.41	1.4	7.4
	0.50	0.32	1.1	5.8
	0.30	0.19	0.7	3.5
PI159k	1.00	0.86	0.6	24.9
	0.60	0.52	0.4	15.0
	0.30	0.26	0.2	7.5
PI211k	1.00	0.74	1.3	24.7
	0.60	0.45	0.8	14.8
	0.30	0.22	0.4	7.4
PI472k	1.00	0.78	1.2	61.3
	0.60	0.47	0.7	36.8
	0.40	0.31	0.5	24.5
	0.24	0.19	0.3	14.7
	0.12	0.09	0.2	7.4
	0.08	0.06	0.1	4.9

[a] ϕ_p = volume fraction of polymer in solution; ϕ_{bb} = volume fraction of polymer that is backbone; Z_{branch} = number of branch entanglements, eq 6; Z_{bb} = number of backbone entanglements, eq 7.

PI211k and PI472k. Of course, this is not surprising, given the fact that the theory is not intended to deal with marginally entangled or unentangled branches. We also recognize that there are some uncertainties in the model regarding the relaxation behavior of the comb architecture and the treatment of polydispersity. For example, the model treats the polydispersity of branch and backbone length as well as the number of branches, but it does not take into account uncertainties in the placement of the branch points[63,79] or the architectural dispersity due to incomplete synthesis.[80,81] However, the most likely conclusion from Figure 6 is that the disparity between the predictions and the data is simply due to the inapplicability of the model for marginally entangled branches.

We argue below that it is not a breakdown of the basic physics of the model that is the problem, but rather the parameter estimation for short branches. In particular, if we examine Figure 6, we see that the relaxation times, corresponding to the number of entanglements listed in Table 1, are under predicted for the combs with short branches. This means that the frictional effect of the short branches on the dynamics of the backbone is also underestimated for the marginally entangled and unentangled systems. This is not at all surprising, given the results of recent studies of three-arm asymmetric stars with two long arms (M_l) and one short arm (M_s). After the short branch of an asymmetric star relaxes, the two remaining long arms resemble a linear chain ($M_{lin} = 2M_l$) with a single branch point at the center. In the tube model, the terminal time of the remaining linear chain is calculated by understanding that the diffusion constant of the backbone is dependent on the fluctuation time of the short branch

$$D_{bb,asym\_star} = \frac{p^2 a^2}{2\tau_{branch}} \tag{16}$$

where a^2 is the backbone tube diameter. The empirical parameter p is introduced as a way to increase the effective friction of the branch point. Although a number of different values of p have been proposed,[39,43,49,63,64] we have previously noted that there is some consensus[11−13] that $p^2 = 1/12$ yields a necessary reduction in the friction when the short branch is still long enough to be entangled.

In a recent study that is relevant to the present work because it included short arms that were very short, Frischknecht et al.[44] compared the linear viscoelastic behavior of a series of asymmetric stars with varying short arm length

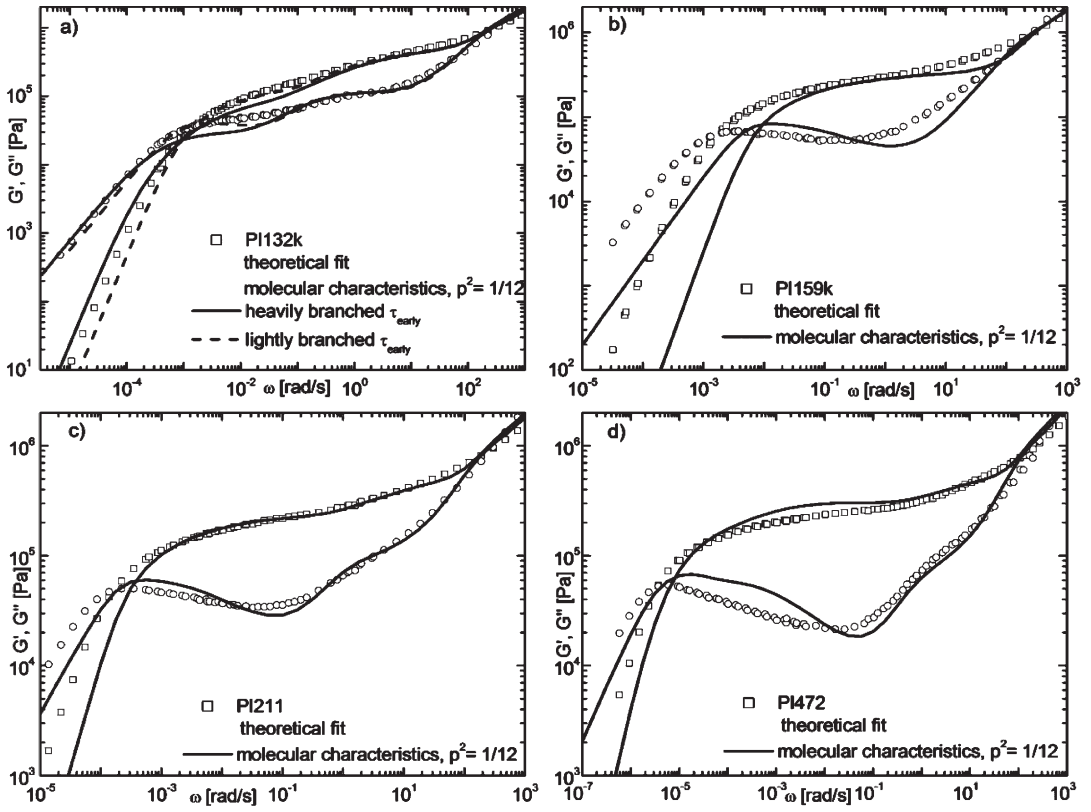

Figure 6. Linear viscoelastic frequency spectra of polyisoprene combs (□, ○) compared with theoretical predictions[11] (—) using molecular characteristics with $p^2 = 1/12$ and $\alpha = 1$: (a) PI132k ($\varepsilon_{bb} = 1.05$, $\varepsilon_{branch} = 1.05$), comparison between lightly branched (---) and heavily branched (—) derivation of τ_{early}. (b) PI159k ($\varepsilon_{bb} = 1.06$, $\varepsilon_{branch} = 1.08$). (c) PI211k ($\varepsilon_{bb} = 1.02$, $\varepsilon_{branch} = 1.02$). (d) PI472k ($\varepsilon_{bb} = 1.04$, $\varepsilon_{branch} = 1.02$).

against a tube model theory in order to ascertain the effect of the short branch. Frischknecht et al. found that the tube model with $p^2 = 1/6$ underestimated the effect of the branch point for the most lightly entangled short branches (2.5 and 4 entanglements) while it correctly predicted the terminal relaxation time for a star with ~10 entanglements on the short branch. Progressively smaller values of p^2 were needed to capture the terminal relaxation behavior of asymmetric stars with lightly entangled branches, indicating that the short arms were creating a larger amount of drag than predicted.

Recently, a coarse-grained simulation of branch point motion in asymmetric star polymers by Zhou and Larson[48] demonstrated that short arms with one or two entanglements had a much higher effective drag than expected, based on the arm retraction (contour length fluctuation) model (which is also incorporated in Kapnistos et al.'s hierarchical model for comb polymers). Simulations of a Rouse chain demonstrated excellent agreement with the molecular dynamics simulation if a decreased value of p^2 were chosen, consistent with the experimental data of Frischknecht et al.[43] Zhou and Larson[48] suggested that the entanglement molecular weight on time scales of τ_e is roughly half of M_e calculated from the plateau modulus, which is why the shorter branches have a higher friction and appear to be effectively more entangled. All of this work on asymmetric stars points strongly to the fact that short branches exert a much stronger frictional "drag" than expected, and that this can be incorporated into a tube theory by either decreasing p^2 or by decreasing the entanglement molecular weight. Of course, at this time, there is no fundamental theoretical basis for choosing between these alternatives or for choosing the value of either p^2 or M_e. Nevertheless, we believe that it is worthwhile to see whether

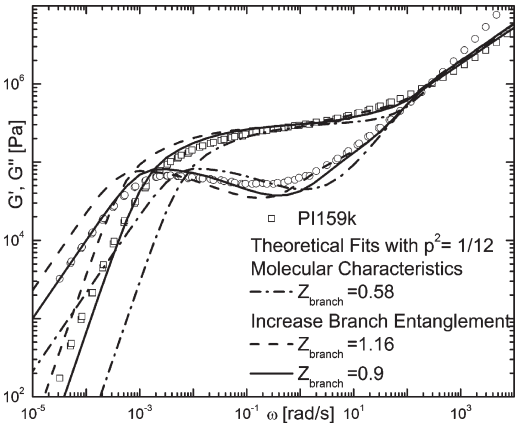

Figure 7. Comparison of experimental linear viscoelastic data for PI159k (□, ○) with Kapnistos et al.[11] model predictions with $p^2 = 1/12$ and different branch entanglement values without polydispersity. Molecular characteristics of comb $Z_{branch} = 0.58$ (-·-), increased branch entanglement on suggestion of Zhou and Larson[48] $Z_{branch} = 1.16$ (---), and best fit with $Z_{branch} = 0.9$ (—).

the predictions of Figure 6 can be improved by applying the Zhou and Larson idea of a reduction in the effective M_e to the branch points of a comb polymer.

Because of the hierarchical relaxation of the comb, we must analyze the effect on both the branch and backbone relaxation, rather than just analyzing the terminal time of the backbone. We begin with the case of PI159k, which has unentangled branches. In particular, we assume that the branch relaxation time scales for use in the Kapnistos et al.[11] model should be calculated by assuming a smaller entanglement molecular weight so that the branch appears as

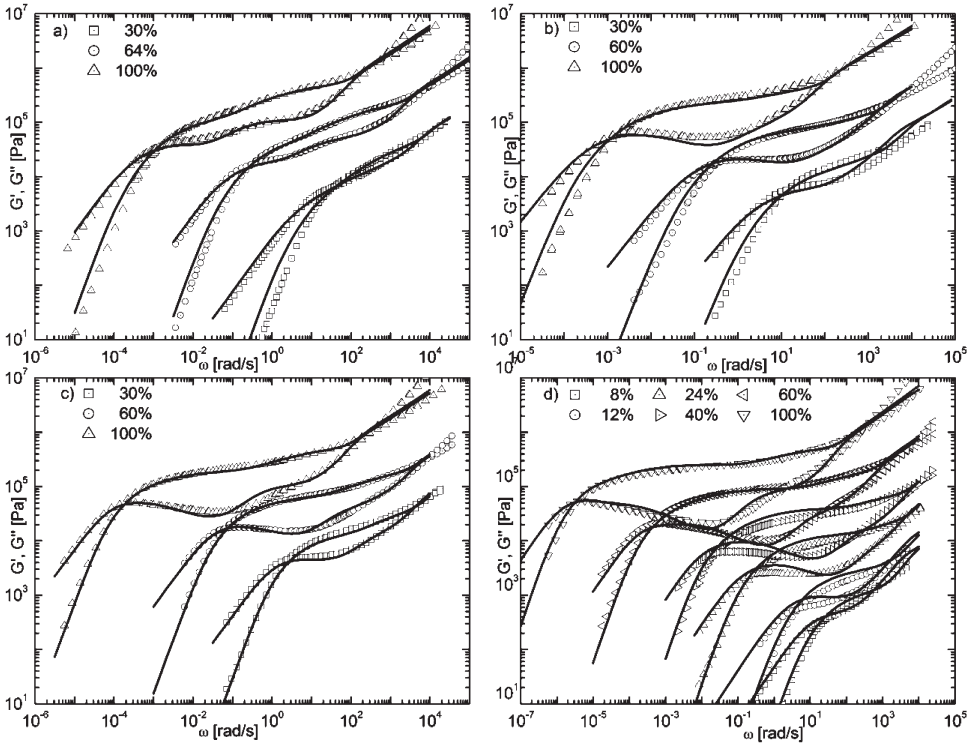

Figure 8. Linear viscoelastic frequency spectra (symbol) for polyisoprene comb polymers at −30 °C compared with Kapnistos et al. model[11] with $p^2 = 1/12$ and $\alpha = 1$: (a) PI132k ($\varepsilon_{bb} = 1.05$, $\varepsilon_{branch} = 1.05$) $\phi = 0.3$ (□), $\phi = 0.64$ (○), and $\phi = 1$ (△) with molecular characteristics and model for lightly branched combs (—). (b) PI159k ($\varepsilon_{bb} = 1.06$, $\varepsilon_{branch} = 1.08$) $\phi = 0.3$ (□), $\phi = 0.6$ (○), and $\phi = 1$ (△) with predictions of $Z_{branch} = 0.9$ (—). (c) PI211k ($\varepsilon_{bb} = 1.02$, $\varepsilon_{branch} = 1.02$) $\phi = 0.3$ (□), $\phi = 0.6$ (○), and $\phi = 1$ (△) with predictions of $Z_{branch} = 1.65$ (—). (d) Selected curves for PI472k ($\varepsilon_{bb} = 1.04$, $\varepsilon_{branch} = 1.02$) $\phi = 0.08$ (□), $\phi = 0.12$ (○), $\phi = 0.24$ (△), $\phi = 0.40$ (right-pointing △), $\phi = 0.60$ (left-pointing △), and $\phi = 1$ (▽) with predictions of $Z_{branch} = 1.62$ (—).

effectively more entangled. Zhou and Larson suggest that for branches that have a molecular weight of $O(M_e)$ or smaller τ_{branch} should be estimated as though the entanglement molecular weight is approximately halved, i.e., $Z_{branch} = M_{branch}/0.5M_e$. The general proposition of using decreased values of M_e (i.e., increased values of τ_{branch}) but with a fixed value of p^2 for comb polymers is tested in Figure 7, for PI159k using several values of M_e (here expressed in terms of the number of entanglements Z_{branch}) ranging from the expected equilibrium value of 0.58.

As shown in Figure 7, increasing the branch relaxation time correctly predicts both the branch and backbone relaxation time scales without changing $p^2 = 1/12$. The fit with the data is best for $Z_{branch} = 0.9$. This is between the value estimated from the equilibrium entanglement molecular weight and the prescription of Zhou and Larson to simply halve M_e. Considering that the relaxation of the weakly entangled branches of combs PI211k and PI472k are also underpredicted by the model (Figure 6), we can rationalize that there should be an increase in the branch entanglement for these cases too (albeit smaller than for PI159k) in order to recover the correct relaxation time for the backbone. The predicted curves are shown in Figure 8. It should be noted, for all of the cases shown in Figure 8, that it is necessary to empirically decrease the values of τ_e beyond the static dilution value $\tau_e = \tau_e^0\phi^{-2\alpha}$ to enable the Kapnistos model to fit the high frequency data for each solution. In effect, this accounts for the fact that τ_e is expected to shift due to the changes in T_g for the solutions as we mix different proportions of squalene and polyisoprene ($T_g \sim -108$ °C[1] for squalene and −61 °C for polyisoprene (Table 1)). When this is done, the model also provides excellent fits for the backbone relaxation process, again for fixed $p^2 = 1/12$.

The model predictions in Figure 8 were created using the branch molecular characteristics, $Z_{branch} = 2.2$, for PI132k (a) and increasing the branch entanglement for PI159k (b), PI211k (c), and PI472k (d) to $Z_{branch} = 0.9$, 1.62, and 1.65, respectively. The overall fit of the experimental data with the model predictions is very promising and with one change captures not only the intermediate but also the terminal time scales correctly with $p^2 = 1/12$. Recall that the alternative method proposed to increase the friction of the short branches by making an empirical change in the parameter p^2 from the value $p^2 = 1/12$. While this method would improve the long-time dynamics of the backbone, it would not provide any change to the intermediate time scales since it does not appear in the relaxation of the branches. The ability to closely model both the branch and relaxation dynamics is important when relating the relaxation time scales to the relaxation behavior from a nonlinear deformation.

4.2. Nonlinear Rheology. The comb polymers are tested in a step shear strain flow to probe the effect of the short branches on the nonlinear stress relaxation behavior of the comb. Nonlinear stress relaxation mastercurves of the entire comb relaxation process, from fast relaxation of the branches to the slower relaxation of the backbone, were created using time−temperature superposition as in Kapnistos et al.[40] The damping behavior is analyzed at short and long times to determine how the architectural characteristics of the comb influence the response to deformation. We examine the behavior of both polymer melts and solutions to study the effect of dilution on the damping behavior of the comb architecture. A complete set of stress relaxation curves for each sample in Table 1 will be available in the Ph.D. dissertation of Kirkwood.[82] We report here two typical sets of data that illustrate qualitatively different behavior.

Selected stress relaxation curves for two of the polyisoprene combs are shown in Figure 9 with time scales from the linear regime noted.

The stress relaxation curves illustrate that there are qualitative similarities between the relaxation of the comb polymer backbone and a well-entangled linear chain (e.g., the dip in the stress relaxation modulus representing a loss of stress due to retraction[16,19,55]). We also notice that there are qualitative differences between the stress relaxation behaviors of the two combs in Figure 9a,b that are likely related to the architectural differences between the combs and the number of backbone entanglements.

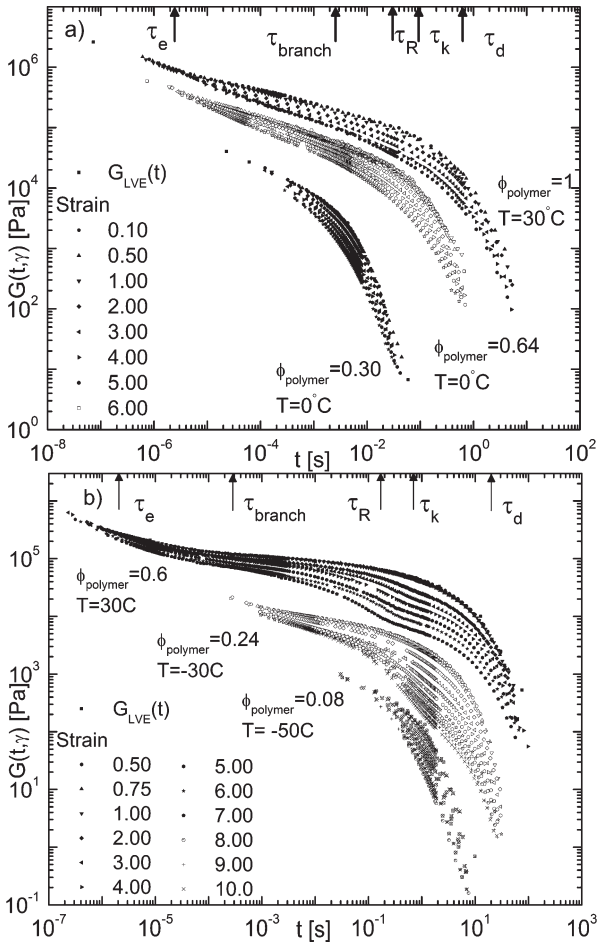

Figure 9. Unshifted stress relaxation mastercurves (a) PI132k at 100% (■), 64% (□), and 30% (crossed □) at $T = 30$, 0, and 0 °C, respectively, and (b) 472k at 60% (■), 24% (□), and 8% (crossed □). For the highest concentration time scales are noted: Rouse time of an entanglement segment, τ_e, longest relaxation time of branch, τ_{branch}, Rouse time of comb backbone, τ_R, and backbone reptation time, τ_d, as well as the characteristic shift time, τ_k.

4.2.1. Damping Behavior at Short Times: Comb Branches. The stress relaxation curves of Figure 9 are shifted at τ_{branch}, the branch relaxation time from the linear viscoelastic model in the preceding section (Figure 8), to calculate the comb damping function on time scales of the branch relaxation, which we refer to as the branch damping function, $h_{branch}(\gamma)$. The shifted stress relaxation curves are shown in Figure 10, and the corresponding values of $h_{branch}(\gamma)$ are plotted in Figure 11, where they can be compared with predictions given by eq 14.

There is some variability in the damping function for the relaxation modulus due to the uncertainty in τ_{branch} for the polyisoprene combs with short branches. Here we use τ_{branch} from Figure 8 to calculate the damping functions for Figure 11. There is also some uncertainty due to the backbone and branch relaxation not being completely decoupled,[40] which is clearly seen in the linear viscoelastic data. The theoretical calculation of the branch damping function assumes that there are two different types of segments: those with free ends that are able to retract on fast time scales and those trapped between branch points that remain stretched on these short time scales. The volume fraction of comb able to retract includes the comb ends, and to estimate $\phi_{retract}$ we assume that the branch points are evenly distributed along the backbone. However, since the branch points are actually randomly distributed, there is some error in determining the value of $\phi_{retract}$ and some uncertainty in the prediction.

The backbone is a large part of these combs (high ϕ_{bb}, low $\phi_{retract}$), and the overall soft damping behavior indicates that the backbones remain stretched and hold a large amount of stress on the short time scale of branch relaxation. Although the short time behavior of the combs is not completely captured by eq 14, the general behavior gives confidence that this approach contains the correct physics for describing the nonlinear relaxation of the branches. Furthermore, the fact that there is reasonable agreement between the data and theory in Figure 11 provides strong evidence that the hierarchical relaxation process persists even in the nonlinear regime. Our knowledge of the relaxation mechanisms

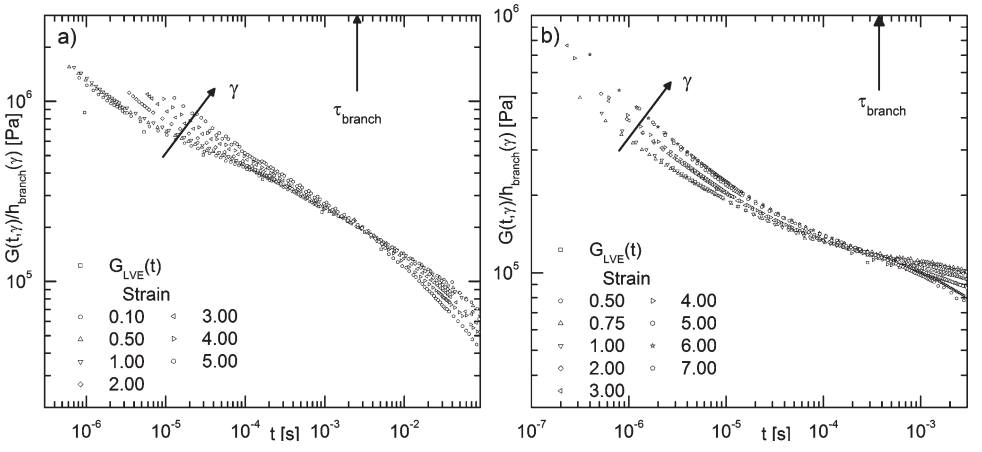

Figure 10. Stress relaxation mastercurves shifted to $G_{LVE}(t)$ from the linear viscoelastic frequency sweep at the branch relaxation time, τ_{branch}, to calculate the branch damping function: (a) PI132k; (b) PI472k60.

and time scales can then be applied to determine the effect of architecture on the longtime backbone damping function.

4.2.2. Damping Function at Long Times: Backbone Damping Function. We can understand the effect of architecture on the stress relaxation behavior by comparing the comb backbone with a linear chain. In the framework of hierarchical relaxation, the backbone is viewed as a linear chain with friction blobs at the branch points that relaxes stress using mechanisms that are the same as a linear chain. The stress relaxation mastercurves are shifted at long times to determine the backbone damping functions (Figure 12).

The characteristic shift times are found to be between τ_R and τ_d of the backbone in all cases (Table 3). This is expected for linear chains as the Rouse time is the time scale of the retraction process after which the linear chain relaxes using the linear viscoelastic mechanisms. For the comb backbone, the fact that τ_k is between τ_R and τ_d indicates that the stress relaxation process could be similar to a linear chain. The results of Kapnistos et al.[40] suggest that this relationship between the time scales is not always obeyed.

4.2.2.1. Effect of Static Dilution. The results of Kapnistos et al.[40] and Vega and Milner[25] were used by them to suggest that the long time damping behavior for a well-entangled comb backbone should be equivalent to the Doi−Edwards theory, and as the number of entanglements decreases, the behavior should become softer toward the unentangled Rouse limit of linear chains ($h(\gamma) = 1$ or with finite extensibility $h(\gamma) < 1$). The number of backbone entanglements (following dynamic dilution) ranged from 1 to 6 in the combs examined by Kapnistos et al. The results suggest that a small variation in entanglement (e.g., $Z_{bb} = 4$ vs 6) should lead to a noticeable difference in the damping behavior of the comb backbone. Thus, in Figure 13 we compare the damping behavior of the PI132k melt ($Z_{bb} = 11.6$) against the behavior of three different PI132k solutions with backbone entanglement values of ranging from 3.5 to 7.4.

The results are interesting for two reasons. First, the damping behavior of the well-entangled comb backbone is substantially removed from the Doi−Edwards theory, and second, the response is independent of concentration in the range studied. Neither of these is consistent with the previous hypotheses on the expected damping behavior of a well-entangled comb backbone. Concentration is expected to play a role in softening the damping function as the time scale separation between retraction and relaxation becomes smaller (weakly entangled systems). Concentration independence of the damping function for such a large range of entanglements suggests that the architecture of the comb fundamentally influences the fraction of initial stress that is not relaxed

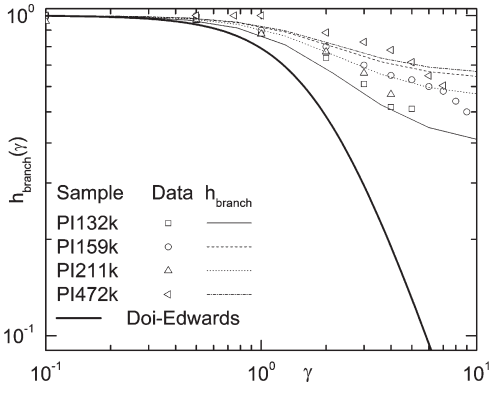

Figure 11. Damping functions calculated by shifting stress relaxation mastercurves to the stress relaxation modulus from linear viscoelastic regime, $G_{LVE}(t)$, at time scales relative to τ_{branch}. Comparison of experimental data (symbols) with short time damping function model (14) (lines) of PI132k (□, ---), PI159k (○, · · ·), PI211k (△, -· ·), and PI472k (left-pointing △, -··-) with Doi−Edwards theory (—), eq 13.

Table 3. Characteristic Time Scales for Selected Combs

sample	ϕ_p	T_{ref} [°C]	$\tau_e \times 10^6$ [s]	τ_{branch} [s]	τ_k [s]	τ_d [s]
PI132k	1.0	30	2.5	0.0025	0.1	0.6
PI132k64	0.64	0	4.00	0.0013	0.05	0.126
PI132k30	0.30	0	1.66	0.00079	0.006	0.0069
PI472k60	0.60	30	2.00	0.00029	0.5	20
PI472k24	0.24	−30	178	0.0053	2.65	27
PI472k08	0.08	−50	7943	0.0028	1.2	5.1

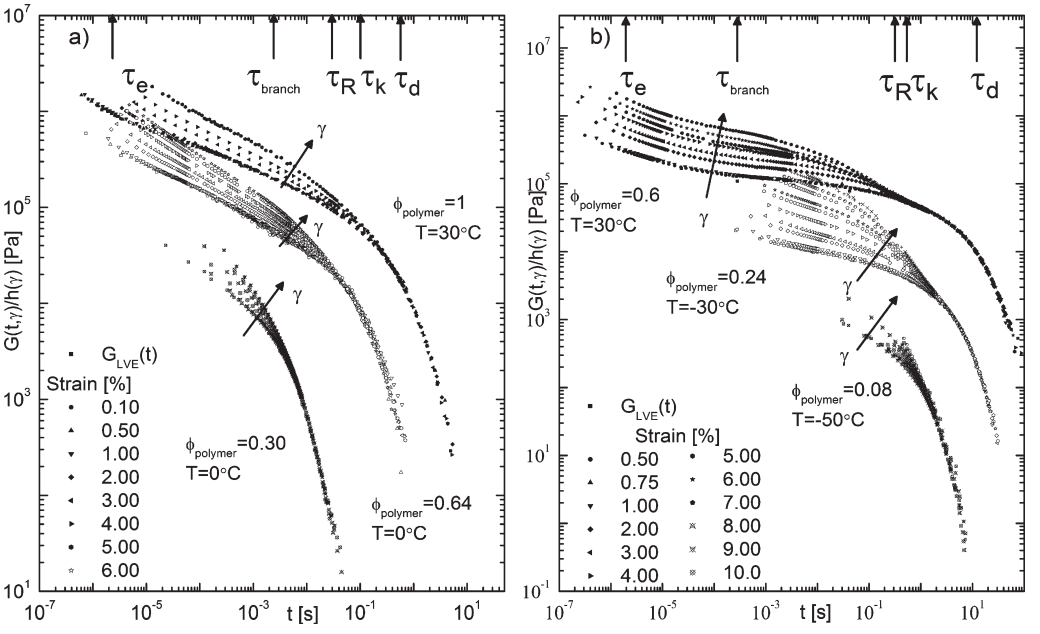

Figure 12. Stress relaxation mastercurves shifted to the stress relaxation modulus from linear viscoelastic regime, $G_{LVE}(t)$, at long times to calculate the backbone damping function: (a) PI132k at 100% (■), 64% (□), and 30% (crossed □) at $T = 30$, 0, and 0 °C, respectively. (b) 472k at 60% (■), 24% (□), and 8% (crossed □). For the highest concentration the time scales from the linear viscoelastic theory are noted.

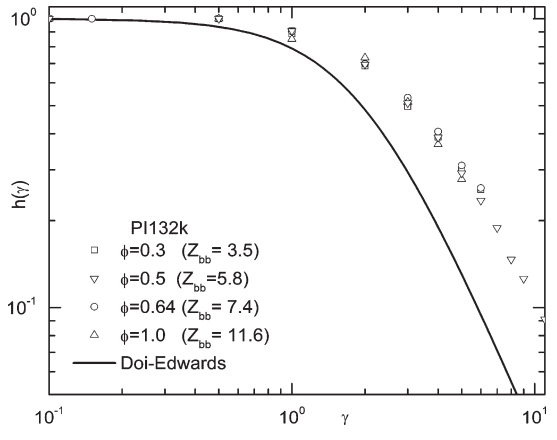

Figure 13. Comparison of long time damping functions of PI132k sample. Calculated number of diluted backbone entanglements Z_{bb} = 3.5 (□), Z_{bb} = 5.8 (▽), Z_{bb} = 7.4 (○), and Z_{bb} = 11.6 (△) compared against the Doi−Edwards theory (—), eq 13.

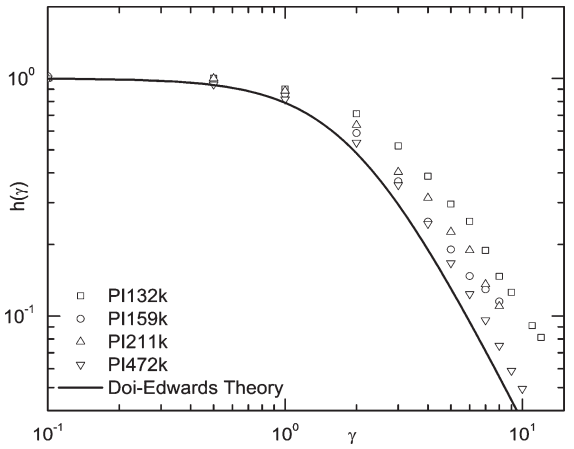

Figure 14. Backbone damping functions calculated by averaging results over multiple concentrations for PI132k (□), PI159k (○), PI211k (△), and PI472k (▽) compared with Doi−Edwards theory (—), eq 13.

before the linear relaxation mechanisms dominate the chain dynamics. The four polyisoprene combs studied all exhibit unique damping functions (Figure 14) independent of concentration when the backbone is more than weakly entangled (i.e., for $Z \geq 3$).

The damping behavior of the combs has weaker strain dependence than the Doi−Edwards theory. To the best of our knowledge, the long time stress relaxation behavior of the backbone assuming full retraction has not been addressed from a theoretical point of view, aside from direct application of the Doi−Edwards theory. In the next section, we will examine how the effects of architecture influence the relaxation behavior of the comb and develop a scaling argument to explain our results.

4.2.2.2. Scaling of Backbone Damping Function for Comb Architectures. We will remain consistent with our understanding of the backbone relaxing as a linear chain in the linear viscoelastic regime and use the Doi−Edwards framework for a linear chain to understand how architecture influences the nonlinear stress relaxation. The presence of the branch points along the backbone inhibits the free motion of the backbone, and under linear deformations the relaxation mechanisms are equivalent to a linear chain with the addition of the friction due to the branch points. Incomplete retraction due to branching has been suggested by Larson[41] as a means to create the softer damping function seen in our comb systems. While this does create a framework to lower the stress lost due to retraction, we have not found a way to relate the architectural parameters of the polyisoprene combs to a mechanism that inhibits retraction and we will proceed assuming that the backbone is able to retract like a linear chain. Another mechanism to describe the softer damping behavior is that the backbone orientation and stretch relaxation occur on the same time scale, like a dilute chain. While this explanation is plausible for lightly entangled polymer chains, it does not seem reasonable for the heavily entangled backbones presented in this study. The experimental data presented in Figure 14 suggest that the damping behavior is dependent on the details of the branching architecture (number and size of branches).

The effect of the branches in the linear viscoelastic regime is to delay the relaxation of the comb backbone (hierarchy of motions) and to dilute the backbone (constraint release−dynamic tube dilution). Both of these "ideas" must be taken into account in order to properly model the linear viscoelastic behavior of the comb backbone, and they will also be used to explain the softer damping response due to comb architecture. The short time damping behavior (Figure 11) demonstrated that hierarchical relaxation persists in the nonlinear deformation regime so that we can assume that the backbone retraction occurs after the relaxation of the branches. We assume that the entire comb is affinely stretched and oriented due to the applied strain, consistent with the Doi−Edwards theory. Immediately after the stretch, on time scales corresponding to the relaxation of the branches, the backbone segments between branch points are unable to retract and therefore remain in the stretched state. While these segments are stretched, chain segments with free ends are assumed to retract. After the comb branches and backbone ends relax, the remaining comb backbone is then free to retract to a more favorable conformation to relieve stress due to the stretched tube. If we concentrate on the backbone, we notice that the tube confining the backbone on time scales of the step imposition is formed by entanglements with branches and other backbones. The relaxation of the branches and backbone ends dilates the diameter of the constraining tube so that when backbone retraction occurs, the backbone is confined to a tube that is dilated relative to the tube in which it was stretched (Figure 15).

We can use the primitive chain framework to show the effect of dilution on the retraction of the comb backbone. Initially there are Z^0_{bb} entanglements along the backbone (with branches and other backbones), and the initial length of the primitive path of the backbone is

$$L_0 = Z^0_{bb} a_0 \tag{17}$$

where a_0 is the tube diameter. Immediately after the step deformation the primitive path of the chain is stretched to length

$$\langle L(t = 0^+) \rangle = \lambda(\gamma) L_0 = \lambda(\gamma) Z^0_{bb} a_0 \tag{18}$$

where $\lambda(\gamma)$ is the chain segment stretch averaged across all possible orientations (Figure 15). However, as the branches and comb ends relax, entanglements with the branches are lost, leaving only the entanglements with other backbones, and the entanglement density of the backbone decreases to

$$Z_{bb} = Z^0_{bb} \phi^1_{BB} \tag{19}$$

assuming the dilution parameter is 1 to correspond to the value used in the linear regime. The volume fraction of

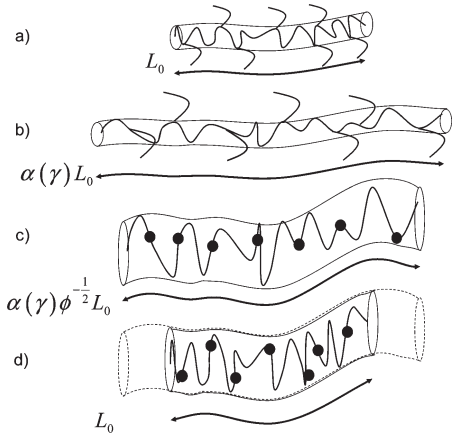

Figure 15. Simplified picture of comb backbone stress relaxation following nonlinear step strain: (a) The comb backbone represented by chain with equilibrium contour length, L_0. Backbone tube is formed from entanglements with other backbones and branches. (b) The imposed step deformation causes affine deformation of the comb backbone primitive chain. The chain contour length increases to $\lambda(\gamma)L_0$. (c) On time scales of τ_{branch}, the branches and backbone ends relax, releasing constraints on backbone. Constraining tube dilates and contour length decreases to $\lambda(\gamma)\phi_{BB}{}^{-1/2}L_0$, where $\phi_{BB}{}^{-1/2}$ is fraction of backbone that is not completely relaxed. (d) On time scales of τ_R, the backbone recovers its equilibrium contour length, L_0. The remaining stress is relaxed through linear relaxation mechanisms.

backbone segments that have not relaxed on time scales of branch relaxation is

$$\phi_{BB} = \frac{M_{bb} - 2x_c M_{bb,end}}{M_{bb} + qM_{branch}} \tag{20}$$

where x_c is the fractional length of backbone end that relaxes on time scales of the branch relaxation.[11] The earlier definition of ϕ_{bb}, eq 8, refers to the volume fraction of backbone segments based on the total number of backbone segments, while ϕ_{BB}, eq 20, is defined as the fraction of backbone segments not relaxed on time scales of branch relaxation. The backbone ends are assumed to relax stretch on short time scales with the branches, but if the backbone end is longer than the branch, only a fraction x_c completely relaxes on time scales of the branch relaxation. This is important for the polyisoprene short branch combs that have backbone ends (assuming equally distributed branches[45,46]) longer than the branches. The relaxation of the branches increases the diameter of the tube and hence the length of each entanglement segment (primitive path) to

$$a = a_0\phi_{BB}{}^{-1/2} \tag{21}$$

with a dilution parameter of 1. The change in tube diameter means that the primitive path length changes to

$$L = Z_{bb}^0 a_0 \phi_{BB}{}^{1/2} \tag{22}$$

due to dilution (Figure 15). On time scales between the branch relaxation and backbone retraction the primitive path of the backbone has changed to

$$\langle L(t = 0^+)\rangle = \lambda(\gamma)\phi_{BB}{}^{1/2}L_0 \tag{23}$$

At this stage, the effective deformation of the backbone from its original length is $\lambda(\gamma)\phi_{BB}{}^{1/2}$ not $\lambda(\gamma)$, which is predicted by the Doi−Edwards theory. The relaxation before backbone retraction modifies the effective strain felt by the backbone before it retracts as a "linear" chain. In order to compare the relaxation behavior of the comb backbone with the Doi−Edwards theory and show that the backbone retracts as if it were a linear chain, we need to scale the strain by the backbone volume fraction. When the damping behavior of the polyisoprene combs is analyzed in the framework described above, good correspondence with the Doi−Edwards theory is observed (Figure 16).

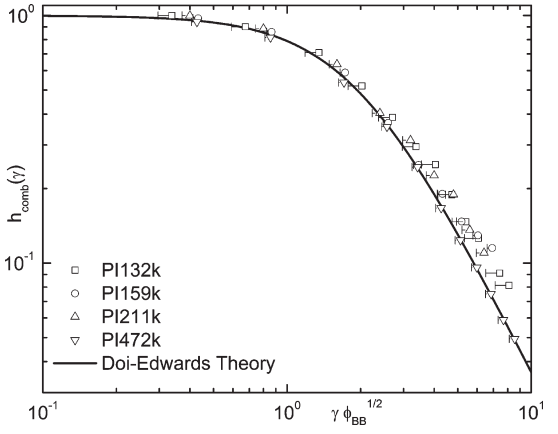

Figure 16. Comparison of experimental backbone damping functions for PI132k (□), PI159k (○), PI211k (△), and PI472k (▽) scaled by backbone dilution to account for relaxation of branches. The Doi−Edwards theory, eq 13, $\phi_{BB} = 1$ (—) is included for reference. Uncertainty bars indicate change in dilution parameter from $\alpha = 1$ to 4/3.

This analysis verifies that the comb backbone is actually retracting as a linear chain, and we recover the Doi−Edwards theory for all of the combs considered in this study with the scaling (23). The scaling of ϕ_{BB} varies depending on the choice of the dilution parameter, and we present the scaled data in Figure 16 with uncertainty bars to show the effect of scaling with $\alpha = 4/3$. We note that experimental neutron spin-echo measurements suggest a scaling of 0.61 for the tube diameter.[1,83] Using the same simplification as Doi−Edwards, an approximation of the damping function for comb architectures is represented by

$$h_{comb}(\gamma, \phi_{BB}) = \frac{1}{1 + \frac{4}{15}\phi_{BB}\gamma^2} \tag{24}$$

The scaling can also be tested by incorporating the data of Kapnistos et al.[40] for long arm polystyrene and polybutadiene combs and of Lee et al.[39] for other polyisoprene combs (Figure 17).

The compiled damping behavior shows good correspondence with the Doi−Edwards theory. The two combs well above the Doi−Edwards curve lc2-PB1k $\phi = 0.5$ (□) and lc1-PB1k $\phi = 0.5$ (tilted ○) are weakly entangled, with only 1 and 2 entanglements after dynamic dilution, and the softer damping behavior would then be expected. The ability to scale the damping behavior of the entangled backbones to the Doi−Edwards curve indicates that the backbone, which we view as a linear chain with friction blobs at the branch points, eventually relaxes like a linear chain.

The backbone retracts, in a tube that is dilated with respect to the tube that initially confined the backbone, to relax stretch on Rouse time scales, and then linear viscoelastic relaxation mechanisms relax the remaining stress on time scales of reptation. This picture of the backbone retracting in a dilated tube requires that hierarchical relaxation persists under the strong nonlinear deformations studied. The damping behavior of the comb at the longest branch relaxation time (Figure 11) was used to demonstrate that the backbone is stretched on time scales of the branch relaxation so that we can assume the comb continues to follow the hierarchy of

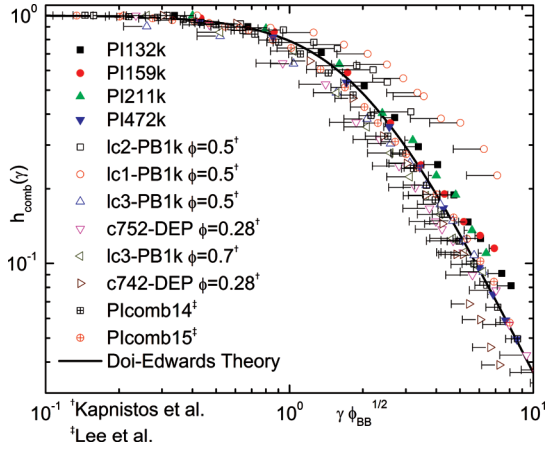

Figure 17. Damping behavior of comb polymers from this study (■) as well as the Kapnistos et al.[40] (□) and Lee et al.[39] (crossed □) scaled by the effect of backbone dilution on the strain and compared against the Doi−Edwards theory (—) (13). Uncertainty bars indicate change in dilution parameter from $\alpha = 1$ to 4/3.

relaxation processes. The comb backbone scaling depends on ϕ_{BB} and the dilution parameter, α. As mentioned earlier, the volume fraction is an approximation because the branch points are randomly dispersed, yet we assume they are evenly placed along the backbone for our calculations. We derived the scaling with a dilution parameter of 1 to correspond with the value used in the linear viscoelastic theory and have included the scaling results for a dilution parameter of 4/3 as an uncertainty bar in the figures. In Figure 17, we notice that the scaled damping behavior for many of the combs sits below the Doi−Edwards prediction. The stronger dependence on strain could be a consequence of an underestimation of the volume fraction due to the assumption of equally distributed branches. It may also reflect the action of the convective constraint release, which was shown by Marrucci and Ianniruberto[84] to predict a damping function below the Doi−Edwards theory. Overall, the scaling of the damping function for the comb backbone demonstrates that we can understand the relaxation of the comb backbone as a linear chain stretched at a lower effective strain due to the relaxation of the branches.

5. Conclusions

We measured the linear rheology of model polyisoprene combs with short branches and well-entangled backbones at a wide range of concentrations. The current understanding of comb relaxation (hierarchy of processes, plus dynamic dilution) was found to even apply to combs with unentangled or weakly entangled branches. We used a sophisticated linear viscoelastic model for entangled comb polymers by Kapnistos et al.[11] to fit the linear viscoelastic behavior of the combs. Previous work on asymmetric stars had shown that the branches with less than two entanglements relaxed as though they were increased in length so that they were effectively more entangled. This idea is further corroborated by the fact that the relaxation behavior of our combs with less than two branch entanglements was fit very well by the Kapnistos model, if we increase the effective entanglement of the branches.

The nonlinear behavior of the polyisoprene combs was studied to clarify the architecture (number and especially size of branches) dependence of the damping function. Recent work hypothesized that the damping behavior for a comb polymer would be equivalent to the Doi−Edwards theory[42] for linear chains if the backbone were well entangled. Through analysis of the short time damping behavior it was determined that hierarchical relaxation persists under the nonlinear deformation. However, the damping function was found to be independent of the number of backbone entanglements (above the weakly entangled limit) and significantly "softer" than the Doi−Edwards prediction, suggesting an architecture dependent response to the deformation.

Simple scaling theory was used to show that the softer damping response exhibited by the comb architecture is a consequence of the dilation of the tube constraining the backbone due to the branch relaxation process. As the tube dilates, the backbone stretch, calculated from the primitive chain length relative to its equilibrium value, decreases from the initial amount corresponding to the macroscopic deformation. If compared to a linear chain, the backbone primitive chain at retraction resembles a linear chain that is deformed at a lower macroscopic strain. Accounting for these changes, we presented a damping function for the comb architecture that correctly captures the behavior of entangled comb polymers from this study as well as previously published experimental data.[25,40]

Acknowledgment. Partial support by the EU (NoE Softcomp NMP3-CT-2004-502235) and the Petroleum Research Fund administered by the ACS (ACS PRF#46399-AC7) is gratefully acknowledged. We thank Tom C. B. McLeish, Hiroshi Watanabe, Ralph Colby, Evelyne van Ruymbeke, and Michael Kapnistos for many useful discussions.

References and Notes

(1) Graessley, W. W. *Polymeric Liquids & Networks: Dynamics and Rheology*; Garland Science: New York, 2008.
(2) McLeish, T. C. B. *Adv. Phys.* **2002**, *51*, 1379–1527.
(3) McLeish, T. C. B. *Curr. Opin. Solid State Mater. Sci.* **1997**, *2*, 678–682.
(4) Roovers, J. *Polymer* **1979**, *20*, 843–849.
(5) Roovers, J.; Graessley, W. W. *Macromolecules* **1981**, *14*, 766–773.
(6) Roovers, J.; Toporowski, P. M. *Macromolecules* **1987**, *20*, 2300–2306.
(7) Ball, R. C.; McLeish, T. C. B. *Macromolecules* **1989**, *22*, 1911–1913.
(8) Marrucci, G. *J. Polym. Sci., Part B: Polym. Phys.* **1985**, *23*, 159–177.
(9) Daniels, D. R.; McLeish, T. C. B.; Crosby, B. J.; Young, R. N.; Fernyhough, C. M. *Macromolecules* **2001**, *34*, 7025–7033.
(10) McLeish, T. C. B. *Europhys. Lett.* **1988**, *6*, 511–516.
(11) Kapnistos, M.; Vlassopoulos, D.; Roovers, J.; Leal, L. G. *Macromolecules* **2005**, *38*, 7852–7862.
(12) Inkson, N. J.; Graham, R. S.; McLeish, T. C. B.; Groves, D. J.; Fernyhough, C. M. *Macromolecules* **2006**, *39*, 4217–4227.
(13) McLeish, T. C. B.; et al.et al. *Macromolecules* **1999**, *32*, 6734–6758.
(14) Although there has been great success in identifying the relevant relaxation mechanisms for the comb architecture in the linear viscoelastic regime,[9,11,12] there are still some conceptual difficulties with the underlying physics used to describe the relaxation. For example, recent work by Watanabe et al. [*Macromolecules* **2002**, *35*, 2339−2357] demonstrated that dielectric relaxation measurements on stars are not described by the physics that are put into the theory, which is also used to describe the comb relaxation. The dielectric relaxation measurements on combs are expected to pose similar problems.
(15) Iza, M.; Bousmina, M. *Rheol. Acta* **2005**, *44*, 372–378.
(16) Islam, M. T.; Sanchez-Reyes, J.; Archer, L. A. *Rheol. Acta* **2003**, *42*, 191–198.
(17) Archer, L. A.; Sanchez-Reyes, J.; Juliani *Macromolecules* **2002**, *35*, 10216–10224.
(18) Ferri, D.; Greco, F. *Macromolecules* **2006**, *39*, 5931–5938.
(19) Osaki, K. *Rheol. Acta* **1993**, *32*, 429–437.
(20) Watanabe, H.; Matsumiya, Y.; Ishida, S.; Takigawa, T.; Yamamoto, T.; Vlassopoulos, D.; Roovers, J. *Macromolecules* **2005**, *38*, 7404–7415.
(21) Vrentas, C. M.; Graessley, W. W. *J. Rheol.* **1982**, *26*, 359–371.
(22) Watanabe, H.; Yao, M. L.; Sato, T.; Osaki, K. *Macromolecules* **1997**, *30*, 5905–5912.
(23) Neidhofer, T.; Sioula, S.; Hadjichristidis, N.; Wilhelm, M. *Macromol. Rapid Commun.* **2004**, *25*, 1921–1926.

(24) Osaki, K; Takatori, E.; Kurata, M.; Watanabe, H.; Yoshida, H.; Kotaka, T. *Macromolecules* **1990**, *23*, 4392–4396.
(25) Vega, D. A.; Milner, S. T. *J. Polym. Sci., Part B: Polym. Phys.* **2007**, *45*, 3117–3136.
(26) Fetters, L. J.; Kiss, A. D.; Pearson, D. S.; Quack, G. F.; Vitus, F. J. *Macromolecules* **1993**, *26*, 647–654.
(27) Takahashi, M.; Nakatsuji, Y.; Ohta, Y.; Masuda, T. Nonlinear stress relaxation of melts of star-branched polystyrenes. In 12th annual meeting of society of rheology Japan, 1985, pp 17−20.
(28) Archer, L. A.; Varshney, S. K. *Macromolecules* **1998**, *31*, 6348–6355.
(29) Bishko, G.; McLeish, T. C. B.; Harlen, O. G.; Larson, R. G. *Phys. Rev. Lett.* **1997**, *79*, 2352–2355.
(30) Chodankar, C. D.; Schieber, J. D.; Venerus, D. C. *Rheol. Acta* **2003**, *42*, 121–131.
(31) Archer, L. A.; Juliani *Macromolecules* **2004**, *37*, 1076–1088.
(32) Islam, M.; Juliani; Archer, L. A.; Varshney, S. K. *Macromolecules* **2001**, *34*, 6438–6449.
(33) Kasehagen, L. J.; Macosko, C. W. *J. Rheol.* **1998**, *42*, 1303–1327.
(34) Bick, D. K.; McLeish, T. C. B. *Phys. Rev. Lett.* **1996**, *76*, 2587–2590.
(35) Larson, R. G. *J. Rheol.* **1985**, *29*, 823–831.
(36) Hepperle, J.; Munstedt, H. *Rheol. Acta* **2006**, *45*, 717–727.
(37) Stadler, F. J.; Auhl, D.; Munstedt, H. *Macromolecules* **2008**, *41*, 3720–3726.
(38) Lee, J. H.; Orfanou, K.; Driva, P.; Iatrou, H.; Hadjichristidis, N.; Lohse, D. J. *Macromolecules* **2008**, *41*, 9165–9178.
(39) Lee, J. H.; Driva, P.; Hadjichristidis, N.; Wright, P. J.; Rucker, S. P.; Lohse, D. J. *Macromolecules* **2009**, *42*, 1392–1399.
(40) Kapnistos, M.; Kirkwood, K. M.; Ramirez, J.; Vlassopoulos, D.; Leal, L. G. *J. Rheol.* **2009**, *53*, 1133–1153.
(41) Larson, R. G. *Constitutive Equations for Polymer Melts and Solutions*; Butterworth-Heinemann: Stoneham, MA, 1988.
(42) Doi, M.; Edwards, S. F. *The Theory of Polymer Dynamics*; Oxford University Press: New York, 1986.
(43) Frischknecht, A. L.; Milner, S. T.; Pryke, A.; Young, R. N.; Hawkins, R.; McLeish, T. C. B. *Macromolecules* **2002**, *35*, 4801–4820.
(44) Graessley, W. W. *Adv. Polym. Sci.* **1974**, *16*, 1–179.
(45) Vazaios, A.; Lohse, D. J.; Hadjichristidis, N. *Macromolecules* **2005**, *38*, 5468–5474.
(46) Vazaios, A.; Hadjichristidis, N. *J. Polym. Sci., Part A: Polym. Chem.* **2005**, *43*, 1038–1048.
(47) Driva, P.; Iatrou, H.; Lohse, D. J.; Hadjichristidis, N. *J. Polym. Sci., Part A: Polym. Chem.* **2005**, *43*, 4070–4078.
(48) Zhou, Q.; Larson, R. G. *Macromolecules* **2007**, *40*, 3443–3449.
(49) Tezel, A. K.; Leal, L. G. *Macromolecules* **2006**, *39*, 4605–4614.
(50) Ferry, J. D. *Viscoelastic Properties of Polymers*, 3rd ed.; Wiley: New York, 1980.
(51) Colby, R. H.; Rubinstein, M. *Macromolecules* **1990**, *23*, 2753–2757.
(52) Kapnistos, M. Linear and Nonlinear Rheology of Architecturally Complex Polymers. Ph.D Dissertation, University of California, Santa Barbara, **2006**.
(53) Zoller, P.; Walsh, D. *Standard Pressure-Volume-Temperature Data for Polymers*; Technomic Publishing Co.: New York, 1995.
(54) Abdel-Goad, M.; Pyckhout-Hintzen, W.; Kahle, S.; Allgaier, J.; Richter, D.; Fetters, L. J. *Macromolecules* **2004**, *37*, 8135–8144.
(55) Gotro, J. T.; Graessley, W. W. *Macromolecules* **1984**, *17*, 2767–2775.
(56) Venerus, D. C. *J. Rheol.* **2005**, *49*, 277–295.
(57) Sanchez-Reyes, J.; Archer, L. A. *Macromolecules* **2002**, *35*, 5194–5202.
(58) Milner, S. T.; McLeish, T. C. B. *Phys. Rev. Lett.* **1998**, *81*, 725–728.
(59) Milner, S. T.; McLeish, T. C. B. *Macromolecules* **1997**, *30*, 2159–2166.
(60) Raju, V. R.; Menezes, E. V.; Marin, G.; Graessley, W. W. *Macromolecules* **1981**, *14*, 1668–1676.
(61) Tao, H.; Huang, C.; Lodge, T. P. *Macromolecules* **1999**, *32*, 1212–1217.
(62) Kapnistos, M.; Koutalas, G.; Hadjichristidis, N.; Roovers, J.; Lohse, D. J.; Vlassopoulos, D. *Rheol. Acta* **2006**, *46*, 273–286.
(63) Lee, J. H.; Fetters, L. J.; Archer, L. A. *Macromolecules* **2005**, *38*, 10763–10771.
(64) Lee, J. H.; Fetters, L. J.; Archer, L. A. *Macromolecules* **2005**, *38*, 4484–4494.
(65) van Ruymbeke, E.; Bailly, C.; Keunings, R.; Vlassopoulos, D. *Macromolecules* **2006**, *39*, 6248–6259.
(66) Wagner, M. H. *Rheol. Acta* **1976**, *15*, 136–142.
(67) Rolon-Garrido, V. H.; Wagner, M. H. *Rheol. Acta* **2009**, *48*, 245–284.
(68) Dealy, J. M.; Larson, R. G. *Structure and Rheology of Molten Polymers*; Hanser Verlag: Munich, 2006.
(69) Isono, Y.; Kamohara, T.; Takano, A.; Kase, T. *Rheol. Acta* **1997**, *36*, 245–251.
(70) Greco, F. *Macromolecules* **2004**, *37*, 10079–10088.
(71) Many authors use the factor 4/15 in the approximation of the Doi−Edwards theory with independent alignment (IA). The numerical solution of DE-IA is actually fit with 0.2, and the factor of 4/15 fits the complete model without IA. The authors thank Jorge Ramirez for pointing this out.
(72) van Ruymbeke, E.; Kapnistos, M.; Vlassopoulos, D.; Huang, T.; Knauss, D. M. *Macromolecules* **2007**, *40*, 1713–1719.
(73) Likhtman, A. E.; McLeish, T. C. B. *Macromolecules* **2002**, *35*, 6332–6343.
(74) Larson, R. G.; Sridhar, T.; Leal, L. G.; McKinley, G. H.; Likhtman, A. E.; McLeish, T. C. B. *J. Rheol.* **2003**, *47*, 809–818.
(75) Fetters, L. J.; Lohse, D. J.; Richter, D.; Witten, T. A.; Zirkel, A. *Macromolecules* **1994**, *27*, 4639–4647.
(76) van Meerveld, J. *Rheol. Acta* **2004**, *43*, 615–623.
(77) Chen, X.; Larson, R. G. *Macromolecules* **2008**, *41*, 6871–6872.
(78) van Ruymbeke, E.; Orfanou, K.; Kapnistos, M.; Iatrou, H.; Pitsikalis, M.; Hadjichristidis, N.; Lohse, D. J.; Vlassopoulos, D. *Macromolecules* **2007**, *40*, 5941–5952.
(79) Das, C.; Inkson, N. J.; Read, D. J.; Kelmanson, M. A.; McLeish, T. C. B. *J. Rheol.* **2006**, *50*, 207–235.
(80) Kirkwood, K. M. Ph.D Dissertation, University of California, Santa Barbara, **2009**.
(81) Richter, D.; Farago, B.; Butera, R.; Fetters, L. J.; Huang, J. S.; Ewen, B. *Macromolecules* **1993**, *26*, 795–804.
(82) Marrucci, G.; Ianniruberto, G. *Philos. Trans. R. Soc. London A* **2003**, *361*, 677–688.
(83) Watanabe, J.; Matsumiya, Y.; van Ruymbeke, E.; Vlassopoulos, D.; Hadjichristidis, N. *Macromolecules* **2008**, *41*, 6110–6124.
(84) Watanabe, H. *Prog. Theor. Phys. Suppl.* **2008**, *175*, 17–26.